Identifying Varicella-Zoster Virus Latent Genomes in an Alternative Neuronal Latency Model

by

Michael Brandon Yee

BA Cell & Molecular Biology, Washington & Jefferson College, 2003

Submitted to the Graduate Faculty of the

Department of Infectious Diseases and Microbiology

Graduate School of Public Health in partial fulfillment

of the requirements for the degree of

Master of Science

University of Pittsburgh

2020

UNIVERSITY OF PITTSBURGH

GRADUATE SCHOOL OF PUBLIC HEALTH

This thesis was presented

by

Michael Brandon Yee

It was defended on

March 31, 2020

and approved by

Vishwajit L. Nimgaonkar, MD, PhD
Professor
Departments of Psychiatry and Human Genetics
School of Medicine, Graduate School of Public Health
University of Pittsburgh

Giovanna Rappocciolo, PhD
Assistant Professor
Department of Infectious Diseases and Microbiology
Graduate School of Public Health
University of Pittsburgh

Thesis Director: Paul R. "Kip" Kinchington, PhD
Professor
Departments of Ophthalmology, Molecular Microbiology and Genetics
School of Medicine
University of Pittsburgh

Paul R. Kinchington, PhD

Identifying Varicella-Zoster Virus Latent Genomes in an Alternative Neuronal Latency Model

Michael Brandon Yee, MS

University of Pittsburgh, 2020

Abstract

Varicella zoster virus (VZV) is the etiologic agent of chickenpox (varicella) upon primary infection and shingles (herpes zoster, HZ) upon reactivation from neuronal latency. Shingles is a debilitating disease of the elderly and immune impaired that is frequently complicated. Reactivation of VZV causing HZ is painful and can result in a chronic pain state known as postherpetic neuralgia (PHN) that is difficult to alleviate. HZ has also been linked to encephalitis, meningitis, vasculopathies and increased risk of stroke, all of which emphasize the continued public health demand for better treatments and/or vaccines. VZV latency and reactivation has not been well characterized because it presents monumental difficulties studying it in a laboratory setting. Its human-specific restriction requires human neuronal platforms for modeling neurotropism, latency and reactivation. Importantly, VZV genomes are found not only in neurons of sensory ganglia, but in those of autonomic, enteric and cranial ganglia, and possibly even the CNS. These latent genomes are difficult to characterize and are usually found only by performing end-stage methods of analyses, when tissues/cells need to be fixed or extracted. One aspect of this research was to explore methods that would better enable the identification of VZV genomes in latently infected cells and whether they could be applied in a live-cell *in vitro* setting. We have previously established that sensory-like neurons derived from human embryonic stem cells (hESC) can host both a productive VZV infection and a model state of VZV latency that can be

experimentally reactivated. However, the maintenance of hESCs and their differentiation into sensory neurons for larger scale applications is exceedingly demanding. The second goal of this research was to evaluate an alternative neuron-like system that is more easily expandable for large-scale applications. We evaluated the proliferative human neuronal precursor cell line Lund human mesencephalic (LUHMES) cells. Differentiated LUHMES can easily be scaled to large numbers and show biochemical, morphological, and functional features of mature neurons. While both undifferentiated and differentiated LUHMES cells are fully permissive to VZV infection, current studies are addressing the potential of this system to host a VZV latent state, and whether this is experimentally reactivatable.

Table of Contents

List of Tables

List of Figures

List of Abbreviations

BAC: Bacterial artificial chromosome

bp: Base-pair

BDNF: Brain-derived neurotrophic factor

bFGF: Basic fibroblast growth factor

BME or **βME**: Beta mercaptoethanol

Brn3a: Brain-specific homeobox/POU domain protein 3A

CNS: Central nervous system

CPE: Cytopathic effect

DAPI: 4′,6-diamidino-2-phenylindole

db-cAMP: Dibutyryl-cyclic adenosine monophosphate

DHFR: Dihydrofolate reductase

DNA: Deoxyribonucleic acid

dpi: Days post-infection

EdU: 5-Ethynyl-2′-deoxyuridine

FBS: Fetal bovine serum

FiSH: Fluorescence *in situ* hybridization

GDNF: Glial cell-derived neurotrophic factor

GFAP: Glial fibrillary acidic protein

GFP: Green fluorescent protein

hESC: Human embryonic stem cell

HIGS: Heat-inactivated goat serum

hpi: Hours post-infection

HSV: Herpes simplex virus

HZ: Herpes zoster

IE: Immediate early

IF: Immunofluorescence

Kan: Kanamycin

LUHMES: Lund human mesencephalic cells

NGF-β: Nerve growth factor beta

NS: Neurosphere

NT-3: Neurotrophin 3

ORF: Open reading frame

PBS: Phosphate buffered saline

PCR: Polymerase chain reaction

PFA: Paraformaldehyde

PFU: Plaque forming units

PDMS: Polydimethylsiloxane

PHN: Postherpetic neuralgia

PI3K: Phosphoinositide 3-kinase

PNS: Peripheral nervous system

pOka: Parent Oka strain

qPCR: Quantitative polymerase chain reaction

RE: Restriction endonuclease

ROCK: Rho-associated, coiled-coil containing protein kinase

RPE: Retinal pigmented epithelium

UL: Unique long

US: Unique short

vOka: Vaccine Oka strain

VZV: Varicella-zoster virus

wpi: Weeks post-infection

Zeo: Zeocin

Preface

I have many people to thank for achieving this academic milestone. To begin with I would like to thank my thesis committee members, Dr. Giovanna Rappocciolo and Dr. Vishwajit Nimgaonkar. Dr. Robbie Mailliard has also provided great guidance over the course of my masters project. I would especially like to thank my thesis director Dr. Paul "Kip" Kinchington. I have not only had the privilege of calling him my boss for the past 16 years, but I have also come to think of him as my friend and mentor. The guidance, wisdom, and knowledge he has bestowed upon me is truly remarkable. He has always shown support, encouragement and consistently provides acknowledgement of my successes and value to our research family, long before I sought to advance my education. The freedom and independence he stresses on lab members has been invaluable to allowing me to flourish as a scientist.

I would like to acknowledge current lab members: Lillian Laemmle, Ben Warner, and Betty Wu. I would also like to thank past lab members I have encountered throughout my lab tenure that have also helped shape me not only as a person but as a scientist: Amie Eisfeld-Fenney, Christina Ferko, Jean-Paul Vergnes, Angela Erazo, Vidya Ramachandran, Jean-Marc Guedon, Sarah Bidula, and Ben Treat. Each and every one of these people have enthusiastically provided me encouragement and guidance during my master's education. I would also like to thank Kira Lathrop of the Image Acquisition and Analysis Module in the Eye and Ear Institute for her guidance and assistance with anything and everything microscopy related.

I would be remiss if I did not thank my family for their support during my academic endeavor. Lastly, I would like to thank my wonderful husband Matt who is the reason I even applied for the program. He had the faith and confidence in me that I lacked in myself and is

continually pushing me to not only be a better person, but a more well-rounded person. I could not have gotten through this without his loving support, which also includes swift kicks in the butt to stay on top of my studies.

1.0 Introduction

1.1 Varicella-Zoster Virus

Varicella-zoster virus (VZV) causes varicella (chickenpox) upon primary infection and herpes-zoster (shingles) following reactivation from neuronal latency. VZV is highly communicable through aerosolized respiratory droplets containing virus or direct contact with skin lesions of an infected individual [1]. Varicella is characterized as an acute, highly contagious disease which presents clinical symptoms following an incubation period of 10-21 days after acquisition [2]. Clinical symptoms associated with varicella include headache, fever, malaise, and a characteristic itchy vesicular rash. VZV gains access to sensory neurons innervating the skin and travels by retrograde axonal transport to the sensory ganglia where it establishes a quiescent, or latent, state for the life of the host [3]. Since the virus has a T-cell-mediated systemic phase during varicella, it has been strongly suggested that this permits the virus to gain access to multiple non-sensory ganglia and even the enteric nervous system [4, 5]. VZV can reactivate from this latent state due to immunosenescence or immunodeficiency to cause a reactivated infection known as herpes-zoster (HZ). During reactivation, the virus replicates within neurons and spreads to other neurons within the same ganglia. The virus then travels by anterograde axonal transport along the nerve fibers innervating the skin to cause a dermatomal vesicular rash. HZ clinical symptoms manifest as radicular pain, itching, increased sensitivity to stimuli causing pain (hyperalgesia), and hypersensitivity to touch (mechanical allodynia) and heat (thermal hyperalgesia). Although the disease resolves within 7-20 days, 10-30% of individuals may experience a persistent debilitating pain state known as postherpetic neuralgia (PHN), which can last for months to decades. Herpes

zoster ophthalmicus (HZO) occurs when a reactivation event occurs in the ophthalmic branch of the trigeminal ganglia. HZO presents as a dermatomal rash on the forehead and can affect any part of the eye from the conjunctiva to the optic nerve [6].

Live-attenuated vaccines are available for both varicella and herpes zoster, Varivax and Zostavax, respectively. Both were made from the same attenuated Oka strain of VZV by serial passaging in guinea pig embryo fibroblasts and then human cell lines. The well-tolerated and highly efficacious varicella vaccine has proven to be 70-90% protective against infection and 90-100% effective against preventing moderate and severe disease [7]. Zostavax contains around 14-fold higher titer of the same Oka strain used in the varicella vaccine. This HZ vaccine has shown to provide a reduction of about 51% in the development of shingles and about a 67% reduction in the development of PHN (measured as the "burden of disease"), but protection appears short lived for only 4-8 years from vaccination [8]. A recent development has been a subunit vaccine, Shingrix, for HZ that has proven to be more than 90% effective at preventing both shingles and PHN. Initial studies suggest it maintains a longer efficacy of protection around 85% protection for at least 4 years [9, 10]. Despite the availability of these vaccines, HZ vaccination coverage is still rather low due to a variety of reasons, with one being a lack of knowledge regarding the possible severity of HZ. This large percentage of the population that remains unvaccinated continue to be at risk for reactivation of wild-type VZV, possible vaccine breakthrough infections, and/or even vaccine-induced HZ. This emphasizes the continued public health concern for VZV.

1.1.1 VZV virology

VZV is a member of the alphaherpesvirinae subfamily of the *Herpesviridae* family. VZV has a double-stranded DNA (dsDNA) genome of 125-kilobase pairs that contains at least 70 unique

open reading frames, or ORFs, of which 5 have no homologs to other herpesviruses [11]. VZV gene expression kinetics are assumed to mirror those of other alphaherpesviruses, such as HSV and pseudorabies virus (PRV), in which immediate early (IE) genes are expressed first in the absence of *de novo* viral protein synthesis. Early (E) genes are transcribed following accumulation of functional IE gene products. Finally, late (L) genes are maximally transcribed only after DNA replication, with some being made at low levels before (L1) and others absolutely requiring DNA replication to start (L2). However, because the virus is extraordinarily cell-associated in *in vitro* culture, it is difficult to obtain high titers of cell-free infectious virus, making it very difficult to experimentally prove this.

Structurally the virus resembles that of other herpesviruses. The linear dsDNA genome is encapsidated by the icosahedral nucleocapsid, which is comprised of 7-12 highly ordered proteins with a symmetrical organization, except for the portal which lies at one vertex [12]. Surrounding this is a proteinaceous tegument layer that contains proteins involved in entry and egress of the capsid, viral transport, virion assembly, and transcriptional regulators of both viral and cellular genes that promote a lytic infection [13]. The outer layer is a host-derived lipid envelope that is studded with viral glycoproteins. The viral proteins on the outer envelope are involved in binding to cells and fusion with the target cell membrane, resulting in viral entry.

1.1.2 VZV latency

The defining characteristics of all alphaherpesviruses is a specific genomic arrangement, a short reproductive cycle, the ability to replicate in a variety of tissues and cells, and the establishment of latency from which virus can reactivate. Most, but not all, alphaherpesviruses establish latency in sensory neurons. It has been proposed that VZV latency in humans should be

defined as the persistence of non-productive repressed viral genomes that can reactivate. This true reactivation can sometimes be confounded by abortive infections in which viral genomes merely persist due to the host cell's lack of ability to allow lytic replication [14].

VZV is an exclusively human-specific virus causing human disease only. One of the issues with VZV biology is that there are currently no animal models that recapitulate the full spectrum of VZV disease, including the induction of a reactivatable latent state. The only models that might apply are the guinea pig, which can host some VZV replication; and a parallel model in monkeys with simian varicella virus (SVV), which is the most related virus to human VZV. There exists, however, a human embryonic stem cell (hESC)-derived neuron platform that has proven to be successful in modeling VZV latency and reactivation [15]. This model, and one like it, closely follows the general mechanism of establishing latency as seen with human disease. That is, virus can infect at the axon tips of neurons and travel by retrograde axonal transport to the cell body, or soma. In human infections, the onset of latency is promoted by infection at the axon termini. During entry into the axons, the tegument proteins are left behind at the fusion point as the virus travels down the axon. As a result, tegument protein transactivators are not delivered to the nucleus [16-18]. Once in the soma the virus becomes quiescent, or latent, and the genome is maintained in an episomal state. This silenced chromatin state is suspected to be maintained by many host cell mechanisms, including the actions of histone deacetylases (HDACs) and phosphatidylinositol-3-kinase (PI3K)-induced signaling pathways. HDACs act to silence gene expression by deacetylation, which promotes a latency-favorable environment. Persistent PI3K signaling from receptor binding by nerve growth factor (NGF) aids in maintaining this latent state.

Experimental latency can also be established by infecting neurons directly with cell-free VZV but with the addition of antiviral drugs, which are used to block initiation of lytic infections.

In such infections the outcome is often a mixture of virus that establishes a latent state upon infection and virus that initiates a lytic infection, which, if left unchecked will take over the culture [19]. A commonly used class of antiviral drugs, known as nucleoside analogs, can promote herpesvirus latency by interfering with DNA replication in lytic infections. These drugs are similar enough to nucleotides that they are preferentially incorporated into the viral genome during DNA replication, but in doing so they result in a chain termination. In published studies, the nucleoside analog acyclovir (ACV) has been most often used but VZV is considerably more resistant to ACV when compared to HSV. One other compound our lab has been exploring is brivudine (BVDU), a nucleoside analog of thymidine that is specifically activated upon phosphorylation by the viral thymidine kinase (TK), but not human TK [20]. This drug is far more effective against VZV than ACV and thus is the antiviral we use to establish latency.

It is thought that because the virus is prevented from replicating its DNA, it becomes silenced by chromatin so that a latent state is established immediately upon infection. Infected neurons can also detect viral nucleic acids via innate sensors and secrete non-cytolytic type I interferon (IFN-I) and proinflammatory cytokines in response, which may inhibit lytic viral replication and promote latency in the local environment. The presence of virus-specific T-cells in VZV-infected ganglia suggests that the actions of the innate and adaptive cellular immune system are controlling the latent state [21]. Furthermore, studies using fetal human dorsal root ganglia (DRG) xenografts transplanted in severe combined immunodeficient (SCID-hu) mice suggests that the VZV infectious process can be modulated solely by innate responses since the animals do not have an adaptive immune response [22].

1.1.3 Reactivation from latency

Full reactivation can be defined as the molecular switch from the repressed viral state to a lytic replication cycle which results in infectious progeny virus. Reactivation in humans is a complex process that is heavily regulated by several cellular factors as well as immunological mechanisms. The *in vitro* reactivation process is a simplified adaptation of some of the key factors involved in maintaining the latent state. This is highlighted by the lack of any type of immune control in *in vitro* latency experiments. However, it is worth considering some of the factors that are thought to regulate reactivation of herpesviruses.

Briefly, one of the more currently accepted models of HSV reactivation involves a two-stage reactivation program [23]. To review, latency is established in nuclei of infected neurons when viral genomes are heavily chromatinated, silencing viral IE gene expression. Chromatinization involves wrapping the viral DNA around histones forming nucleosomes, which play an important role in both transcriptional activation and repression. Because neurons are non-dividing, the cells remain alive and the viral genomes are maintained in a silent state. Phase I, or animation, is initiated when neuronal stress response pathways are activated, which in turn activates the c-Jun N-terminal kinase (JNK) pathway by other cellular mediators. This results in the phosphorylation of histones, leading to derepression of the genome which allows chromatin to become more permissive for transcription. A general burst of viral IE, E, and L gene transcription results in *de novo* synthesis of several viral proteins. The transcription of viral genes during phase I does not follow the widely accepted cascade of viral gene expression seen in acute lytic infections. Repressive viral factors and/or innate immune responses may also be triggered during this phase, in which case the viral genome will be silenced, and latency is established once again. If sufficient quantities of key viral proteins are made during phase I, a second wave of viral gene

expression occurs (phase II, or reactivation) in the typical cascade of gene expression, which results in the amplification of viral DNA and assembly of infectious virus. This two-stage reactivation model for HSV can theoretically be applied to VZV. This model further emphasizes why cellular immunity plays such an important role in preventing reactivation and HZ.

Latent infections can be experimentally reactivated in *in vitro* cultures. A common reactivation stimulus is the application of HDAC inhibitors, such as sodium butyrate (NaB), which reverses the silencing mechanism of HDACs, leading to hyperacetylation of histones. This creates an environment that is more favorable for transcription in general, permitting the genome to be derepressed, leading to lytic replication, resulting in infectious virus particles [24].

The repressive actions of PI3K signaling can also be reversed by the addition of the PI3K-inhibitor LY294002 [25]. When NGF binds to its receptor TrkA it initiates cellular signaling through PI3-K which maintains chromatin repression states, therefore the addition of LY and/or NGF withdrawal should result in increased viral replication [15]. When switching to this permissive lytic state, histone acetyl transferases acetylate histones, which reduces their DNA binding and condensation. This action reduces the repressive state of the genome and permits access by transcription factors and allows viral gene expression to proceed. Some groups have also used an NGF-specific antibody to deplete the NGF in cultures to induce reactivation [26]. An issue is that this reduces the NGF signaling that is necessary to maintain the viability of the neurons.

1.1.4 Challenges of working with VZV

VZV infectivity is highly cell-associated and produces very little infectious extracellular virus in culture. The basis of this has eluded investigators because fluid taken from varicella

lesions contain highly infectious cell-free virus. When cells are lysed, infectious virus not only remains bound to membrane components, but also becomes unstable and loses titer rapidly. Cryopreservation of infectious virus stocks requires that all cells in the culture dish, infected and uninfected, are trypsinized and frozen as intact cells using classical cell freezing media containing 10% DMSO. This is unlike virus isolation from HSV infected cells, where large amounts of mature HSV virions are present in the cytoplasm of infected cells and are released from the infected cell into the media. Harvesting high titer HSV only requires freeze/thaw cycles to lyse the cells, releasing even more virus into the media, with free virus preparations greater than 5×10^9 PFU/ml being easily obtained. It is not known why the VZV infectious particle to virion ratio is extremely low (around 1 in 10^6), while for HSV it is around 1 in 100 [27]. A possible explanation is that in VZV, the envelope is acquired by budding through cellular vesicles that may be formed by the induction of the initial steps of autophagy [28]. While the freeze/thaw method will lyse the cells, the large amounts of virus bound to cellular membranes/debris presents challenges for any immunofluorescence studies, since these membrane components are often full of antigen. While cell-free VZV preparations are possible, the methods are rather laborious and require large amounts of infected cell cultures which still yield very low and unstable titers. Viral kinetics studies are difficult to assess because a synchronous infection cannot be performed since cell-free titers are rarely above 10^5/ml. The virus particles in the infecting cells are at all stages of replication making it difficult to assess timing of viral kinetics. Finally, high host cell specificity remains one of the major challenges of working with VZV in a laboratory setting. While VZV in humans exhibits broad tissue tropism (epithelial, keratinocyte, T cell, sebocyte, monocyte, endothelial, Langerhans and PBMC) [29], the host cell range in the experimental setting is more restricted.

1.2 Neuron Model Systems

1.2.1 hESC-derived neurons

The use of hESC-derived neurons has become a critical tool in studying VZV latency and reactivation as they allow the study of VZV in its natural reservoir of latency, the human neuron. hESCs can be differentiated into any number of cell types provided the right signals for differentiation pathways are provided, but more specifically, a multitude of neuronal phenotypes have been developed by differentiation. Neurons with characteristics of peripheral sensory neurons can be derived through this platform making them an ideal model for virus-neuron interaction studies including axonal transport [30]. However, the differentiation process gives rise to a heterogeneous neuron population (a mix of sensory and CNS-like neurons) which requires further investigation and careful identification of the desired peripheral neurons.

1.2.2 Non-hESC derived neuron culture systems

Excised human fetal ganglia offer a viable alternative platform for VZV studies, but many ethical issues exist along with the added challenge of obtaining fresh neuronal tissues for culture. While some studies have shown that VZV can propagate in these neurons in culture, latency and reactivation have not been convincingly demonstrated [31-33]. Alternatively, human cadaveric ganglia have been used to study some aspects of VZV latency. Because much of the population has been previously infected with HSV and/or VZV, most of these ganglia may already harbor latent virus, making it difficult to establish a nascent infection *in vitro*. These studies, however, have substantiated the presence of the VZV latency-associated transcript (VLT) and ORF63

transcripts in human latency [34], and moreover have shown that the latent genome is circular and episomal [35]. One aspect that has not yet been achieved with dissociated or intact cadaveric ganglia is reactivation of latent virus resulting in production of infectious virus [36].

Neuron-like cells called SH-SY5Y have been derived from bone marrow biopsies from a neuroblastoma patient. These cells can be terminally differentiated into neuron-like cells in which VZV replicates and exhibits intracellular spread [37], but a reactivatable latent infection has not been reported. In addition, SH-SY5Y neurons lack many characteristics of mature adult human ganglionic neurons.

Lastly, the SCID-hu mouse *in vivo* model which contains human fetal ganglia xenografts examines human neurons in a system in which glia and satellite cells can interact with the implanted ganglia to assess VZV pathogenesis [38, 39]. Studies have reported that VZV genomes have persisted in the xenografts for months, suggesting a latent infection has been established. However, to date, there have not been any reports of reactivation of VZV in these persistently infected grafts, leading to speculation that these could possibly be abortive infections. It is clear that further expansion of this model is necessary to gain further knowledge into VZV neurotropism.

2.0 Public Health Significance and Statement of Purpose

While clinical manifestations of VZV disease have been reduced with the introduction of vaccines for both varicella and HZ, the incidence of VZV diseases, in particular HZ, is likely to persist for quite some time. There are around a million cases of HZ each year in the US, with over one third becoming complicated by long term sequelae. Most adults still harbor wild-type VZV in their ganglia with the potential to reactivate to cause HZ, and a lifetime risk of disease is estimated to be 20-35% [40, 41]. Both shingles vaccines have low coverage for multiple reasons. Increased disease risk and complications are ever-present in the immunocompromised/immune-suppressed population including individuals with cancers or HIV/AIDS, transplant recipients on immunosuppressive therapies, and pregnant women. While VZV does respond to antivirals, treatment must be initiated very rapidly after onset of rash to be effective. As such, it is likely that HZ and its complications will be an important public health concern for years to come.

While VZV lies dormant in the sensory ganglia of the host for life, we still know very little about the latent state of this virus. We argue that knowledge of the latent state will permit us to identify targets during latency that can be eventually developed to prevent reactivation.

A gap in our knowledge stems from the fact that the current hESC-neuron models of latency are still quite inefficient, and only a small fraction of neurons become latently infected [15]. This makes the analyses of whole latently infected neuron cultures difficult, because signatures from the few latent neurons are difficult to distinguish from the vast majority of uninfected neurons. Our ultimate goal is to be able to compare the transcriptional events occurring in a latently VZV-infected neuron to those of uninfected neurons. Are there specific subtypes of neurons that are preferentially infected like in many HSV models [42]? Does latency influence

the host transcription program? Can latently-infected neurons be selected and concentrated? What does the VZV latent genome make during latency? So far, latent genomes have been identified using fluorescence *in situ* hybridization (FiSH) [15], and for this system it requires cell fixation and isopycnic isolation of nuclei, followed by an extensive FiSH protocol. That approach does not tell us much more than the fraction of neurons that are VZV positive and where the genome signature resides in the nucleus. The first aim of this project seeks to overcome this knowledge gap by developing methods to directly label viral genomes. The first approach was to test the possibility of labeling genomes in a live-cell environment which allows subsequent analyses of virus-host interactions. The second method to detect viral genomes does require fixation of the cells, but all cellular structures remain intact and nuclei do not need to be isolated.

The gap in knowledge for the second aim is that while we currently have utilized the hESC-derived neuron platform to give us fairly pure human neuron populations, the methodologies employed in obtaining these neurons is quite tedious and time-consuming, and requires a high level of technical skill and expertise. This model has taken us years to adapt and optimize, and while generating extensively large hESC-derived neuron cultures is not insurmountable, it is inefficient at best. The second aim of this work sought to explore alternative neuronal model systems that are not only simpler to establish and expand, but also determine whether such systems are permissive for VZV and/or can host a model latent state of VZV and mirror the successes seen thus far with the hESC-derived neuron model. This aim will also extend to assessing the ability to study viral latency and reactivation in this alternative model system.

3.0 Specific Aims

3.1 Aim 1: Development of Methods to Identify VZV Genomes in Latently Infected Cells

This aim sought to explore new methods to identify latent viral genomes in both infected cell cultures as well as neuron cultures. Two different approaches were used to address this issue that involves both the live-cell environment as well as fixed cells.

3.1.1 Aim 1A: An approach for live-cell detection of viral genomes utilizing the *tet*O/TetR-GFP system

Few methods exist that will allow for detection of viral genomes in a latent infection due to the simple fact that during latency the virus becomes inactive and no longer makes detectable proteins or nascent genomes. While viral proteins can be tagged with fluorescent proteins which allows for direct detection of live virus during a lytic infection, they are not made in detectable quantities once latency is established. Moreover, identification of the infected cell becomes difficult while maintaining live cell status. The approach was to develop a recombinant virus which employs the tetracycline operator/tetracycline-repressor (*tet*O/TetR) system. This repressor-operator system has been used to visualize incoming HSV genomes by showing the close association of viral genomes with promyelocytic leukemia nuclear bodies (PML or ND10) and their development into discrete replication compartments [43]. In that report, the authors transfected an amplicon plasmid containing both the TetR and *tet*O elements and then infected with a helper HSV-1 virus to visualize the auto-fluorescent genomes. The amplicon plasmid

contained viral packaging signals, a CMV promoter driving expression of EYFP or EGFP fused to a nuclear localization sequence and the TetR protein, an HSV-1 OriS replication origin, and tandem repeats of the *tet*O sequence. The amplicon plasmid would only be replicated when the helper HSV-1 virus was present in the same nucleus, and the progeny HSV particles would contain the tandem *tet*O repeats and TetR protein. Infectious virus particles harvested from these cells were used to infect new cells, and through time-lapse fluorescent imaging they were able to visualize the incoming viral genomes. This provided the framework for us to exploit this system to visualize VZV genomes in living cells. In the amplicon plasmid system, expression of the Tet components was transient. For our purposes, however, we wanted to have both Tet components expressed in the VZV itself, negating the need for exogenous plasmids.

The plan was to make a recombinant virus engineered to encode 112 tandem repeats of the *tet*O genetic elements, and that also expresses the TetR protein fused to GFP under a strong constitutive promoter. The TetR-GFP encoded by the virus would not be part of the virion or its essential genes, so it should exist as freely diffusing protein within the infected cell. The TetR-GFP protein expression would be inserted at the VZV ORF2 and 3 intergenic region. ORFs 2 and 3 are transcribed in opposite directions to this region of interest, thus insertion of transgenes here will not affect any viral promoters. The cassette containing 112 tandem copies of the *tet*O genetic element would be inserted at the large intergenic gap between ORF60 and 61, which would also not interfere with any viral promoters. The rationale behind this system was that the free TetR-GFP proteins will specifically bind to the *tet*O elements in the viral genome resulting in fluorescently labeled viral genomes that can be visualized in real-time lytic infections. We hypothesized that while the virus itself would be shut down during latency, the TetR-GFP protein made from the strong constitutive CMV IE promoter should remain in the cell and bind to its

target, the *tet*O elements in the viral genome. In effect we hoped this method would mirror the results obtained with FiSH, but theoretically label the genome in a live-cell environment that does not require any further manipulation or addition of extraneous reagents.

3.1.2 Aim 1B: Labeling of VZV genomes with click chemistry modifiable nucleotides

In theory, the establishment of latent genomes in our hESC neuron system comes from the infecting virus, since lytic replication is prevented naturally (by infecting from axonal tips) [26] or by antivirals when the infection is initiated at the neuronal soma. The logic of this approach was to use the thymidine analog 5-Ethynyl-2′-deoxyuridine (EdU), which is incorporated into replicating DNA in dividing cells and the replicating viral genome. This method will be used to incorporate EdU into newly infected, replicating VZV-infected cell cultures so that virus progeny that is harvested (as well as uninfected cells) will all contain DNA with incorporated EdU. Infectious preparations of this EdU-labeled virus can then be used to infect new cells or neurons in which we experimentally induce latency. The genomes that have incorporated EdU should be able to be detected by click chemistry. While the method does involve fixation of the cells, it does maintain the cellular integrity of the neurons that FiSH does not yet provide.

3.2 Aim 2: Modeling Viral Latency and Reactivation Using Alternative Systems to hESC-Derived Neurons

The goal of this aim was to develop an alternative, and easily expandable, neuron culture system derived from a CNS neuronal cell line to use alongside the well-established hESC-derived

neuron culture system so that the biochemistry of latency be investigated. This alternative platform involved the culturing of LUHMES cells and differentiating them into post-mitotic neurons to study neuronal latency, productive replication and reactivation in an easily scalable culture system.

3.2.1 Aim 2A: Establishing permissiveness of LUHMES cells to VZV infection

A recent report has demonstrated that LUHMES-derived neurons are susceptible to HSV-1 infection and can host a latent state that can be experimentally reactivated [44]. HSV-1 is a closely related alphaherpesvirus to VZV, but it has a very broad tropism, infecting most mammalian cells. Therefore, our goal here is to model this recent success using VZV and extrapolating similar datasets exemplified with our hESC-derived neuron system. However, VZV is more growth restricted compared to HSV and far fewer cell lines can host viral growth *in vitro*. Establishing that VZV can replicate in this cell line is paramount to proceeding with any further experiments. We will first determine if mitotically active undifferentiated LUHMES cells can support a lytic VZV infection by utilizing fluorescently labeled VZV to monitor spread of virus between cells. This can then be extended to the use of post-mitotic differentiated neurons derived from LUHMES cells to determine if a lytic infection can be initiated.

3.2.2 Aim 2B: Establishment of latency in LUHMES neurons

Following up on the confirmation of lytic VZV infection, we will then seek to establish a latent infection in LUHMES neurons. Initial experiments will utilize qPCR methods to differentiate latent from lytic genomes. The native structure of the VZV genome in the virion and in the actively replicating lytic infected cell is predominantly a linear form. During latency, the

VZV genome circularizes and becomes episomal by ligation of the genome ends. In recent years qPCR methods have been developed that allow for the detection of and distinction between linear and circular viral genomes [26]. The method utilizes oligonucleotides specific for an internal region of the VZV genome (ORF49), which should yield a PCR product from all genomes; and oligonucleotides specific for fused genomic termini (TR), which should amplify quantifiable products only from cells in which the genome has circularized or has formed a concatemer. Absolute copy numbers determined from each of the reactions will be used to calculate the ratio of fused termini to internal viral sequences (TR/ORF49 ratio). A ratio of 1 will mean there are equal levels of genomic forms, indicating that the virus is not actively replicating. A ratio of less than one means that there are higher levels of linear genomes present than are circular forms, indicative of an actively replicating lytic infection. It is important to note that circular genomes will also be present, albeit in much lower levels, during lytic infection due to the proposed rolling circle model of replication. This method will be used not only to assess the validity of LUHMES neurons as a model for VZV latency and reactivation, but also to assess the ability of viral mutants with genes knocked out to establish latency in future experiments.

Latent infections will be established using the antiviral compound brivudine to block lytic infections. The qPCR data will confirm whether latent infections are supported by LUHMES neurons. If these neurons can indeed support a latent infection, we can then assess whether the latent virus can be reactivated by using the HDAC inhibitor sodium butyrate and/or PI3K-inhibitor.

4.0 Materials and Methods

4.1 Cell Culture

4.1.1 Standard cell culture

All cells lines used were purchased commercially from ATCC unless otherwise noted and all culture media/reagents were purchased from Life Technologies unless otherwise stated. MeWo and MRC5 cells were maintained in Minimum Essential Medium (MEM) supplemented with 10% fetal bovine serum (FBS) (Atlanta Biologicals) and Antibiotics/Antimycotics (Anti/Anti) solution consisting of 100 units/ml of penicillin, 100 μg/ml of streptomycin, and 0.25 μg/ml of amphotericin B. Retinal pigmented epithelial (RPE) cells were maintained in Dulbecco's Modified Eagle Medium/Nutrient Mixture F-12 (DMEM/F-12) supplemented with 10% FBS and Anti/Anti.

4.1.2 Viruses

All viruses used were based on the VZV Parent of Oka (pOka), the clinical varicella isolate that was used as the basis for the varicella vaccine. The VZV pOka genome was maintained in a bacterial artificial chromosome [17] which was manipulated using previously published markerless Red-recombination methods [45]. We discovered two mutations in the original pOka BAC which were corrected via Red-recombination (Yee and Kinchington, unpublished data). This repaired construct served as the parental backbone for all subsequent recombinant virus generation. For generating recombinant viruses, 2.5 μg of purified BAC DNAs were transfected into MeWo

cells with Lipofectamine 3000 (Life Tech) along with 100 ng each of CMV61 and CMV62 plasmid DNAs. VZV IE61 and IE62 are viral transcriptional transactivators that were cloned into expression plasmids under the constitutive CMV promoter. The transient expression of these proteins aids in replication of the transfected viral genome, resulting in faster generation of infectious virus. Without the addition of these plasmids, viral replication would initially be reliant solely on cellular transcription machinery. Infected cell cultures showing 90% cytopathic effect (cpe) were mitotically inhibited by the addition of mitomycin C, to prevent cells from replicating, for 3 hours prior to harvesting the cells for cryopreservation.

VZV with EGFP fused to the amino terminus of the late protein encoded by ORF23 was described previously [19]. Cell-free VZV was prepared as previously described [46].

The parental plasmids containing TetR-GFP and the *tet*O repeat elements were a kind gift from Benedikt Kaufer (Free University of Berlin, Institute of Virology). The BACs were maintained in an *E. coli* strain, known as GS1783, that contains chromosomally encoded Red- and I-SceI-expression under inducible promoters [47]. For the *tet*O/TetR-GFP genome tagging construct, a recombinant BAC was generated to contain mCherry fused to the small capsid protein encoded by ORF23, inserted with a removable kanamycin cassette that was subsequently removed. Next, the TetR-GFP sequence was inserted in the non-essential intergenic region between ORFs 2 and 3 with a Zeocin (zeo) selection cassette. We attempted to PCR amplify the entire multimeric *tet*O sequence with no success. The *tet*O cassette was then removed from the parental plasmid, BB505, and sub-cloned into a pUC19 vector that contained homologous sequences to the intergenic region between ORFs 60 and 61 in the VZV genome, where we were inserting the cassette. This vector was linearized and inserted into the parental BAC which contained mCherry-ORF23 and the TetR-GFP-Zeo cassette. A schematic of the construct is shown in Figure 1.

Purified BAC DNA was transfected, as mentioned above, to generate viruses which expressed TetR-GFP (VZV-mCherry-ORF23_TetR-GFP) and TetR-GFP/TetO (VZV-mCherry-ORF23_TetR-GFP_TetO).

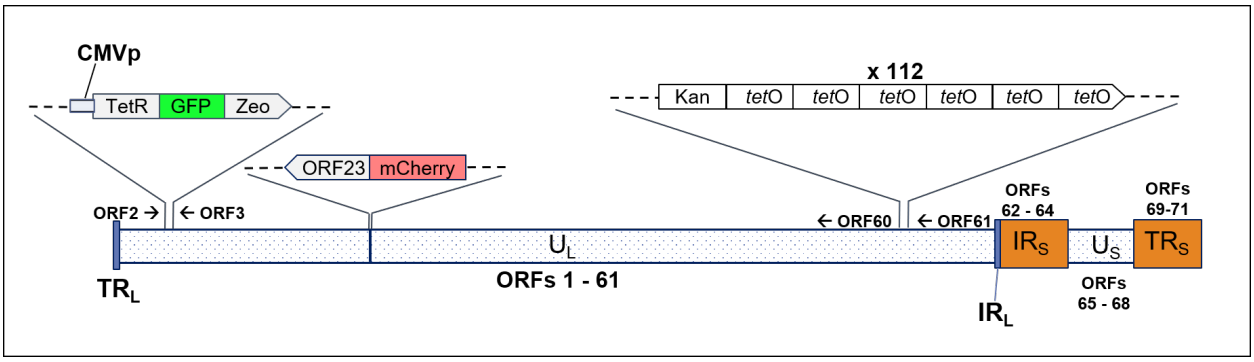

Figure 1. Recombinant VZV Genome Schematic.

4.1.2.1 EdU-labeling and detection

RPE cells were infected with VZV.GFP-ORF23 and then incubated with 10 μM EdU for 48 hours to allow for the replicating infected cells to uptake and incorporate the thymidine analog into the cellular and viral genomes. When the cells were showing 90% cpe, mitomycin C was added to the cells for 3 hours and the cells were harvested and cryopreserved. Virus stocks were then used to infect uninfected RPE or MRC5 cells or neurons. Cells were fixed with 4% paraformaldehyde 24 hpi and the Click-iT Plus EdU Cell Proliferation Kit for Imaging, Alexa Fluor 555 dye (Life Tech.) kit was used to detect the EdU label following manufacturer's protocol.

4.1.3 Stem cell culture and differentiation into neurons

The H9 human embryonic stem cells (hESCs, WiCell) were cultured using both feeder-dependent and feeder-independent methods. Feeder-dependent culture methods used 'hESC Medium' consisting of KnockOut™ DMEM/F-12 medium supplemented with GlutaMax

Supplement, 20% KnockOut™ Serum Replacement (KSR, Life Tech.), 1% non-essential amino acids (NEAAs), 20 ng/ml basic fibroblast growth factor (bFGF, Shenandoah Biotechnology) and 100 μM 2-mercaptoethanol (2-ME, Life Tech.) and Anti/Anti. Feeder-independent culture medium used was StemFlex™ Medium supplemented with StemFlex™ Supplement and Anti/Anti. Following passage by either method, ROCK inhibitor Y-27632 was added to the culture media for 24 hours to increase cell survival rates.

For feeder-dependent culture, γ-irradiated CF-1 mouse embryonic fibroblast (MEF) cells (Applied StemCell) were maintained in DMEM supplemented with 10% FBS, 1% NEAAs, and Anti/Anti. MEFs were plated the day prior to initiating hESC co-cultures. The H9 cells were thawed, briefly centrifuged at 850 rpm for 5 minutes, and resuspended in hESC Medium. The H9 cells were co-cultured with MEF cells in hESC medium with daily medium changes until homogeneous undifferentiated colonies were large enough to passage. Colonies were manually dissected and dislodged from the monolayer under microscope in a laminar flow hood and passaged as clumps.

Feeder-independent cultures were initiated on a 6-well dish pre-coated with GelTrex Basement Membrane Mix (Life Tech). Colonies were passaged either by manual dissection or using ReLeSR™ Enzyme-free cell selection and passaging reagent (STEMCELL Tech.) per manufacturer's instructions.

To generate neural precursor cells (NPCs), H9 cells were co-cultured with the PA6 mouse stromal fibroblast cell line (RIKKEN BioResource Center). The day prior to co-culture, dishes pre-coated with 0.1% Gelatin were seeded with PA6 cells in DMEM with 10% FBS, 1% NEAAs, and Anti/Anti. Before addition of H9 cells, the PA6 cells were rinsed 3X with PBS to remove any residual FBS. H9 cells were then co-cultured with PA6 cells in stromal-derived inducing activity

(SDIA) medium (Glasgow's MEM (GMEM) supplemented with 10% KSR, 1 mM sodium pyruvate, 1% NEAAs, 100 μM 2-ME, and Anti/Anti) for 10-14 days, with medium changes every third day. NPC colonies were manually dislodged using a stereo dissecting microscope into the medium, centrifuged at 850 rpm for 5 minutes, and resuspended in Neurogenic Medium [48] (Neurobasal medium, B-27 Supplement, 10 ng/ml each of NGF, NT-3, and BDNF, and Anti/Anti) and transferred to low-adhesion suspension culture plates. The NPCs were differentiated as floating spheres (neurospheres, NS) for 7-10 days. The spheres were then added to culture dishes coated sequentially with Poly-D Lysine (PDL) and GelTrex and allowed to terminally differentiate for 10-14 days in Neuron Medium (Neurogenic Medium supplemented with CultureOne (Life Tech) to reduce the number of proliferating glial progenitors).

4.1.4 LUHMES cell culture

Undifferentiated Lund Human Mesencephalic (LUHMES) cells were cultured on dishes sequentially coated with poly-L-ornithine (PLO) and fibronectin or as 3D spheres in suspension culture dishes. Basal medium for culture was Advanced DMEM/F-12 supplemented with N2 Supplement (Life Tech.) and Anti/Anti. For routine maintenance and passage of LUHMES cells in an undifferentiated state, basal medium was supplemented with 40 ng/ml bFGF. Post-mitotic LUHMES cells were maintained on PDL-GelTrex coated culture dishes in basal medium supplemented with 1 μg/ml tetracycline or doxycycline, 1mM dibutyryl cyclic AMP (db-cAMP), 2 ng/ml GDNF, 10μM Nardosinone, and Anti/Anti.

4.2 Microfluidics Devices

We manufactured microfluidics devices with two compartments connected by micro channels. We fabricated our own silicon-based master in cleanroom conditions. In brief, silicon wafers (University Wafer) were spin-coated with SU-8 2002 Photoresist (Microchem) in a 2-step process and soft baked. An array of microchannels (10-15 µm wide; 450 µm long; 2-2.5 µm high) was defined by UV light exposure and development of SU-8. Standard soft lithography was performed using Sylgard 184 polydimethylsiloxane (PDMS; Dow Corning). The SU-8/silicon master was first silanized to prevent PDMS from adhering to the master. Because of the restrictive height (2.5 µm) in the channels, cells should be unable to migrate through the channels, but diffusion of small molecules is not impeded. Schematics are shown in Figure 2.

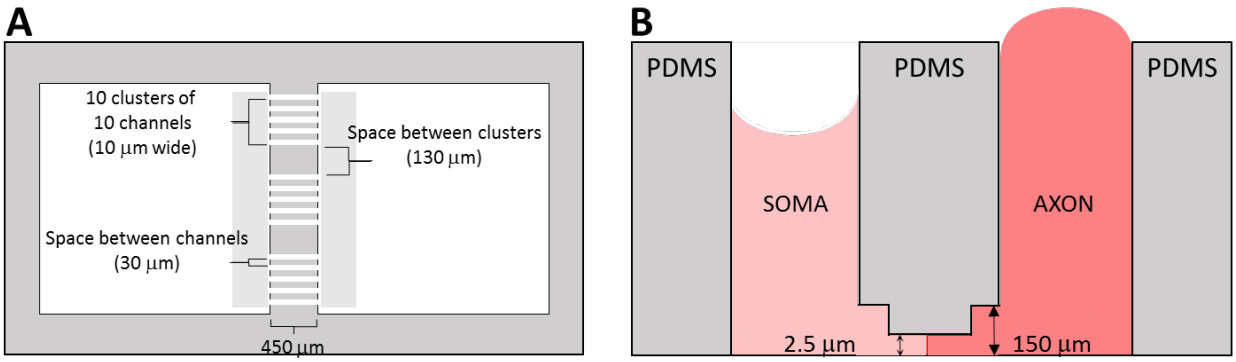

Figure 2. Dimensions of PDMS microfluidics devices and establishment of hydrostatic pressure gradient.

Panel A shows the measurements of each channel (10 µm), the distance between each channel (30 µm), the distance between each cluster of 10 channels (130 µm), and the length of the channels from chamber to chamber (450 µm). The lighter gray boxes on either side of the channels represent the 150 µm "shelf" shown in B that allows the seeding of neurospheres close to the channels. Panel B shows a cross-section of a PDMS device with the appropriate media levels to achieve the hydrostatic pressure gradient and measurements of channel and shelf heights.

4.2.1 Axon isolation using microfluidics devices

PDMS microfluidics devices were permanently bonded to glass substrates using a PE-25 plasma cleaner (Plasma Etch). PDMS and glass substrate were exposed to plasma for 2 minutes at a flow rate of 5 cc/min under 200 mTorr vacuum pressure and then the plasma-exposed surfaces immediately brought together. The chambers of the devices were coated sequentially with PDL and GelTrex before the addition of cells to the "Soma" (cell-body) chamber of the device.

For hESC-derived neurons, the medium for the Soma chamber is the same Neuron Medium formulation described previously. The Axon medium uses the same Neuron Medium with 10-fold higher NGF concentration to attract axons from the Soma chamber to the Axon chamber. Neurospheres were seeded onto the Soma side close to the channels and filled with Soma medium to just under the top of the chamber (Figure 2B). Axon medium was added to the axon chamber to a level that forms a bubble above the top of the chamber to create a dual hydrostatic pressure and NGF concentration gradient. Axonal projections were allowed to extend through the micro channels and into the Axon chamber (7-14 days).

For LUHMES-derived neurons, Soma medium was Advanced DMEM/F-12 with N2 supplement, 1μg/ml doxycycline, 1mM db-cAMP, 2 ng/ml GDNF, 10μM Nardosinone, and Anti/Anti. The medium for the Axon compartment was the same formulation but with 10-fold higher concentrations of doxycycline, db-cAMP, GDNF, and Nardosinone.

4.2.1.1 Retrograde axonal infection

Once axons have projected into the Axon chamber, mitotically inhibited cell-associated or cell-free VZV was added to the Axon compartment. At this stage the pressure gradient was switched to the Soma side (i.e. higher medium level in Soma compartment) to further prevent the

possibility of free virus or cell debris from flowing through the channels and into the Soma chamber. The NGF gradient was also removed so that both chambers contained the same medium with the same concentration of growth factors. Latent infections in the neuron soma should be established by at least 14 dpi following axonal infection [15].

4.3 Immunofluorescence and Microscopy

Cell monolayers (RPE or MRC5) to be analyzed were washed with PBS without calcium and magnesium ($Ca^{++}Mg^{++}$), fixed in 4% paraformaldehyde (PFA) for 20 minutes, washed in PBS, permeabilized with 0.2% Triton X-100 for 5 minutes, and blocked for at least one hour in 10% heat-inactivated goat serum (HIGS). Neurons to be analyzed were washed with PBS containing $Ca^{++}Mg^{++}$, fixed for 30 minutes in 4% paraformaldehyde, washed in PBS without $Ca^{++}Mg^{++}$, and permeabilized with 0.5% Triton X-100/1% Tween-20 in PBS for 2 x 10 minutes. Permeabilized cells were then blocked in 10% (HIGS) in PBS for at least one hour. All antibody incubations were performed in 10% HIGS. Primary antibodies used were rabbit anti-VZV-IE62 and anti-VZV-ORF29 (produced in-house); mouse antibodies to VZV ORFs 29 and 62 (Center for Proteomics, University of Rijeka); chicken anti-beta tubulin III (Novus Biologicals); rabbit anti-Brn3A and mouse anti-GFAP (EMD Millipore); and rabbit anti-peripherin (Neuromics). All secondary antibodies used were produced in goats and conjugated to Alexa Fluor dyes (Life Tech.). Nuclei were visualized by incubating with the DNA-binding dyes Hoechst 33342 or DAPI (Life Tech.).

Images were taken on an Olympus Fluoview 1000 line scanning confocal microscope and analyzed using Fiji image analysis software.

4.4 DNA/RNA Isolation and Quantitative PCR

4.4.1 DNA and RNA isolation for detection of VZV genomes

Cells were harvested for DNA and RNA simultaneously using the Quick-DNA/RNA Miniprep Kit (Zymo Research) following the manufacturer's protocol.

4.4.2 qPCR for VZV DNA configuration

VZV-pOka BAC DNA in which the viral genomic termini are fused was used as a control for episomal (circular) viral DNA. DNA isolated from cell-free VZV-pOka was used to determine copy numbers for linear viral DNA without fused termini. Primers used in this work are listed in Table 1. Real-time qPCR was performed using PowerUp™ SYBR™ Green Master Mix with a StepOnePlus™ Real-Time PCR System (Applied Biosystems™). Primers directed to ORF49 were used to determine copy number of linear viral genomes. Episomal DNA was measured using primers directed to the terminal fusion region. VZV-pOka BAC DNA was used to generate a standard curve for circular genomes. DNA isolated from cell-free VZV-pOka was used to generate a standard curve for linear genomes. The ratio of the absolute copy number of viral PCR products amplified from termini primers to internal primers was calculated. Absolute copy number was determined based on standard curves derived from 10^1 to 10^6 copies of full-length VZV-pOka BAC DNA. The qPCR conditions were as follows: 50°C for 2 minutes, 95°C hot start for 5 minutes; 45 cycles of 95°C for 15 seconds, 58°C for 10 seconds, and 72°C for 45 seconds. Dissociation curve analysis from 60 to 95°C was performed after every qPCR run to exclude nonspecific amplification and formation of primer-dimers.

Table 1. qPCR primers used for viral DNA configuration.

Target	Primer	Sequence
ORF49 (putative late)	ORF49-F21	5′- CGG TCG AGG AGG AAT CTG TG - 3′
	ORF49-R80	5′- CCG TTG CAC GTA ACA AGC TC - 3′
Fused termini	T1	5′- AGT GTC TGT CTG TCT GTG CG - 3′
	T2	5′- CGC GGG TTT TGT TAA AGG CT - 3′

4.5 Southern Blot

The parental plasmid BB505, which contains the *tet*O cassete, and genomic DNA isolated from MeWo cells in which BB505 was transfected, were digested with two restriction endonucleases (REs), XhoI and Tth111I and separated by gel electrophoresis. BAC DNA isolated from bacteria and genomic DNA (gDNA) isolated from VZV-infected cells was also digested with the same enzymes and run on the same gel as the control. The agarose gel containing the DNA fragments was denatured in a solution of 1.5M NaCl/0.5M NaOH at pH 13, neutralized in a solution of 1.5M NaCl/1M Tris-HCl at pH 7.5, and transferred by capillary action in a high salt buffer (20X SSC) to a highly-positively charged nylon membrane. The membrane was cross-linked using a Stratagene Stratalinker UV-Crosslinker, blocked, and probed with an oligo specific to the *tet*O sequence labeled with an infrared dye (5'-IRDye800). Following several stringency washes, the membrane was imaged using a Li-Cor Odyssey Infrared Imaging System.

5.0 Results

5.1 Aim 1: Development of Methods to Identify VZV Genomes in Latently Infected Cells

5.1.1 Aim 1A: An approach for live-cell detection of viral genomes utilizing the *tet*O/TetR-GFP system

Tandem repeats of *tet*O elements are unstable in BAC and VZV constructs.

Generating and characterizing the *tet*O/TetR-GFP virus proved to be very difficult and time-consuming. Several sub-cloning intermediates were necessary to ensure the *tet*O insert contained the proper homology arms to recombine into the pOka BAC. In our initial approach, we inserted the *tet*O-kan-in cassette into the parental BAC (already containing mCherry-ORF23) first, followed by removal of the kan cassette. Then we recombined in the TetR-GFP-kan-in cassette. We encountered issues getting the TetR-GFP-kan-in cassette to recombine into the BAC, so we re-engineered the cassette to encode for the non-removeable Zeocin resistance gene instead of kan. Restriction length polymorphism (RFLP) analysis confirmed the insertion of both the *tet*O and TetR-GFP mutations based on known sequences and expected fragment sizes, and viable virus was generated from the BAC. During lytic infection of MRC5 cells we observed TetR-GFP signal primarily localized in the nucleus (Figure 3A), as expected, where the viral DNA containing the *tet*O elements is replicated and maintained. However, we did not observe TetR-GFP signal localizing to the sub-nuclear replication compartments as expected. Treatment of the cells, before and after infection, with the antivirals acyclovir (ACV) and Cidofivir (CDV) should prevent viral replication, thus driving the virus into a quiescent state where the genomes will be localized in

sub-nuclear compartments. While the latency-like conditions closely reflected this expected localization, the diffuse nuclear GFP signal (Figure 3B) should have diminished, leaving only few GFP puncta as has been observed with FiSH [15]. Because this expected phenotype was not observed (even out to 120 hpi), we further analyzed these constructs by Southern blot with a *tet*O-sequence-specific probe. The results of the Southern blot indicated that the inserted repeats were not the correct length (Figure 4). The restriction enzyme (RE) XhoI (fragments outlined in red) was chosen because it cuts in the 95bp spacer sequence between 6 tandem *tet*O elements, resulting in multiple 347bp fragments (Figure 4, indicated above genome schematic). The 7kb fragment from VZV.mCh23_TetO_TetR represents the genomic region preceding the start of the *tet*O cassette plus the first 6 tandem repeat sequences. However, the 347bp fragments are barely detectable in both the BAC DNA and viral genomic DNA (gDNA), suggesting that the *tet*O sequences were largely deleted. Although the input levels of BAC plasmid DNA appear quite low in the XhoI lane, the lack of 347bp fragments still indicates that the sequences were deleted in the bacterial clone before virus was generated. The Tth111I RE (fragments outlined in black) was chosen because it digests at either end of the entire 112-tandem repeat sequence (indicated below the genome schematic). In the parental plasmid, there is only one site for Tth111I which should result in linearization of the DNA, and as such only a single band should be present. However, this 11.6kb expected fragment is degraded to several smaller fragments. Digestion of the recombinant BAC and VZV-infected cell gDNA with Tth111I should have resulted in a 9.7kb fragment, but this was reduced by about 4.5kb in the BAC and by 5.5kb in the virus. Because recombination was induced to remove the kan-cassette from the *tet*O cassette, and a second time to insert the TetR-GFP-Zeo fragment, we speculated that the large *tet*O cassette may have been

subjected to too many rounds of recombination to generate the dual-expression virus resulting in large deletions.

We then generated a second dual-expression virus, but this time the TetR-GFP-Zeo cassette was inserted first. Because the zeo cassette was not removeable, there was only a second round of recombination induced to insert the *tet*O-Kan-in. The kan-in cassette was in-frame with the rest of the genome sequences and did not interfere with the *tet*O sequences, so another recombination event was not necessary to remove the kan. RFLP analysis again confirmed the correct size fragments were present in the BAC DNA (Figure 5A), and viable virus was generated from this construct. Southern blotting of the new construct revealed that the *tet*O cassette remained intact in the BAC DNA this time, but the virus generated from the BAC again deleted a large portion of the tandem repeats (Figure 5B). The Tth111I digest confirms the full-length *tet*O cassette was maintained in the BAC DNA, but around 4kb of the *tet*O sequence was deleted in the virus. Although equivalent amounts of all DNAs were digested, the signal levels of the parental plasmid BB505 digests were not as strong as the previous blot suggesting some technical discrepancies. Immunofluorescence staining was performed on MRC5 cells infected with the TetR-GFP single expression virus (Figure 3C), which displayed expected generalized GFP signal since the TetR-GFP protein does not have a specific target to bind to. MRC5 cells infected with the new dual-expression virus were probed for the VZV ORF29 protein (Figure 3D). The protein encoded by ORF29 is a single-stranded DNA (ssDNA) binding protein that has been found in human ganglia harboring latent VZV genomes [49], and is predominantly localized to the nucleus of infected cells *in vitro* as it is closely associated with the viral genome during replication [50]. We expected to see co-localization of TetR-GFP with the ORF29 protein, however, they appeared to juxtapose one another in the nucleus. It appears that the TetR-GFP protein is being sequestered into sub-nuclear

compartments, and it doesn't seem to associate directly with the other viral proteins. We speculate that perhaps some *tet*O elements are still intact in the viral genome, but there may be too few of them to produce visible GFP foci or they might be deleted or degraded in such a way that the TetR-GFP protein doesn't recognize them.

These results indicate that the repeat elements are unstable in both the bacteria and the virus. The repetitive sequences are likely being degraded or deleted due to homologous recombination in both the bacteria and in mammalian cells. While it may appear that this is not a viable method for tagging latent genomes in live cells, further development is necessary.

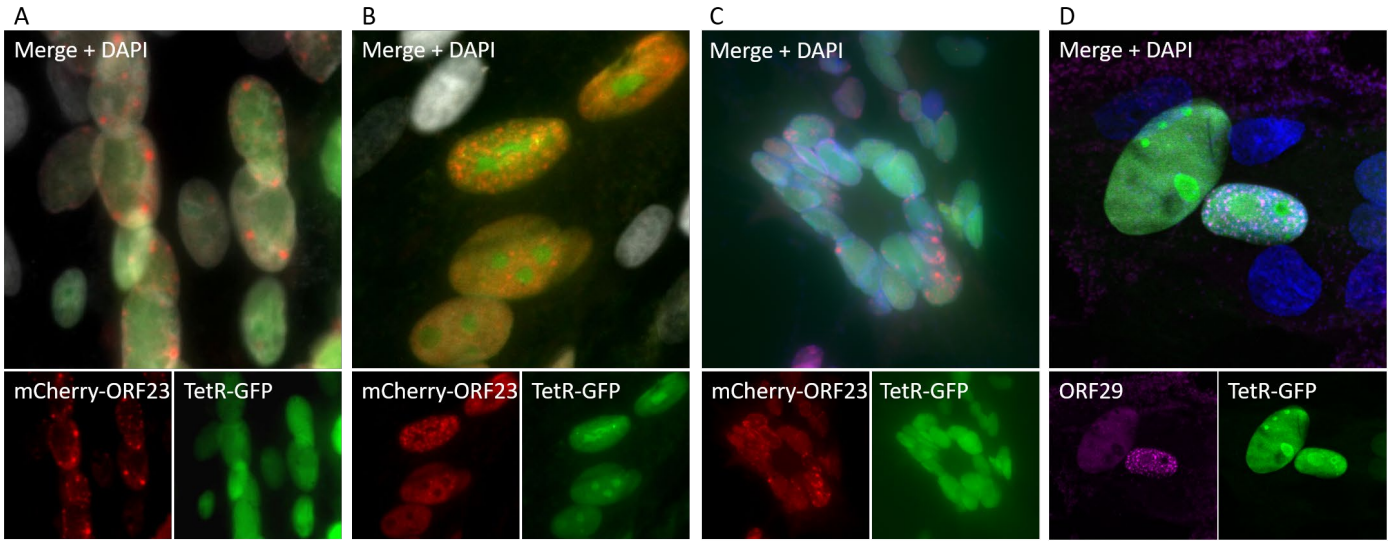

Figure 3. Cellular localization of TetR-GFP and in infected MRC5 cells.

MRC5 cells were infected with the first version of the dual-expression virus (A and B) and with the second version of virus expressing TetR-GFP alone (C) and expressing both TetR-GFP and *tet*O elements (D) and fixed at 48 hpi. (A) Lytic infection shows primarily nuclear localization of TetR-GFP with some cytoplasmic distribution. (B) Experimental latency-like infection displays strictly nuclear distribution with several distinct foci within the nucleus. (C) Cells infected with virus expressing only the TetR-GFP without *tet*O showing generalized GFP signal. (D) Cells infected with dual-expression virus displayed juxtaposing GFP and ORF29 localizations. Nuclei were counterstained with DAPI and are displayed as either white or blue. Images taken 40X (A, B, & D) and 20X (C).

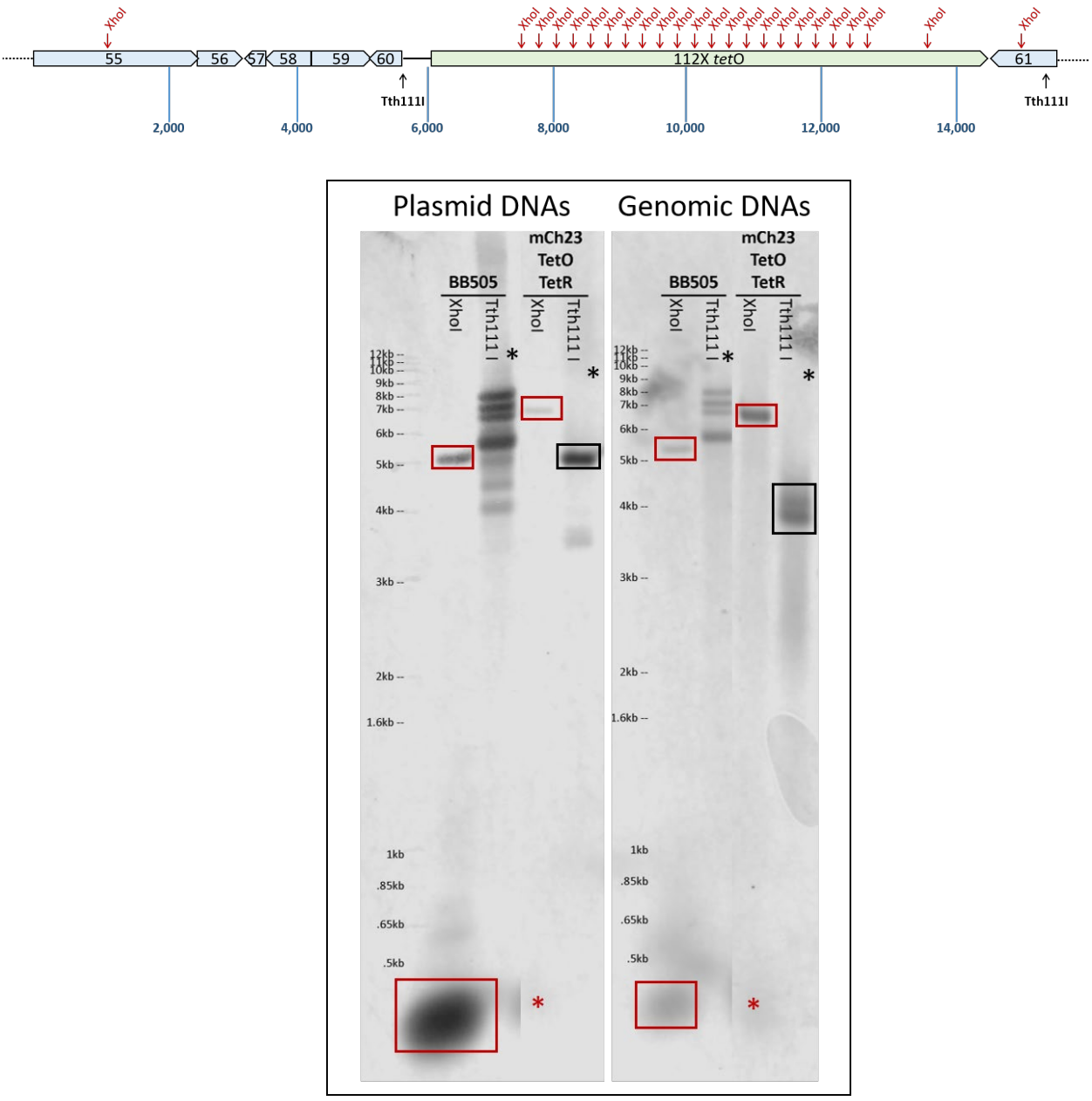

Figure 4. Southern blot of BAC and VZV genomic DNA reveals that the *tet*O DNA repeat elements are unstable.

The genome schematic does not display the entire VZV genome, only the regions that are pertinent to the Southern blot. The numbers in the blue boxes represent the ORFs in the genome and the blue tick marks and numbers below the genome indicate relative sizes and do not correspond to their position in the genome. XhoI cut sites are indicated above the genome in red text and Tth111I cut sites are indicated below the genome in black text. The Southern blot represents cropped sections of the full blot for simplification. A 42 base oligo probe with a 5'-IRDye800 label was used to detect *tet*O sequences. BB505 is the parental plasmid containing the *tet*O-Kan-in cassette. Red boxes indicate XhoI fragments containing *tet*O sequences. Black boxes indicate Tth111I fragments containing *tet*O sequences. Asterisks (*) denote expected DNA fragment sizes and are color coded for the indicated RE.

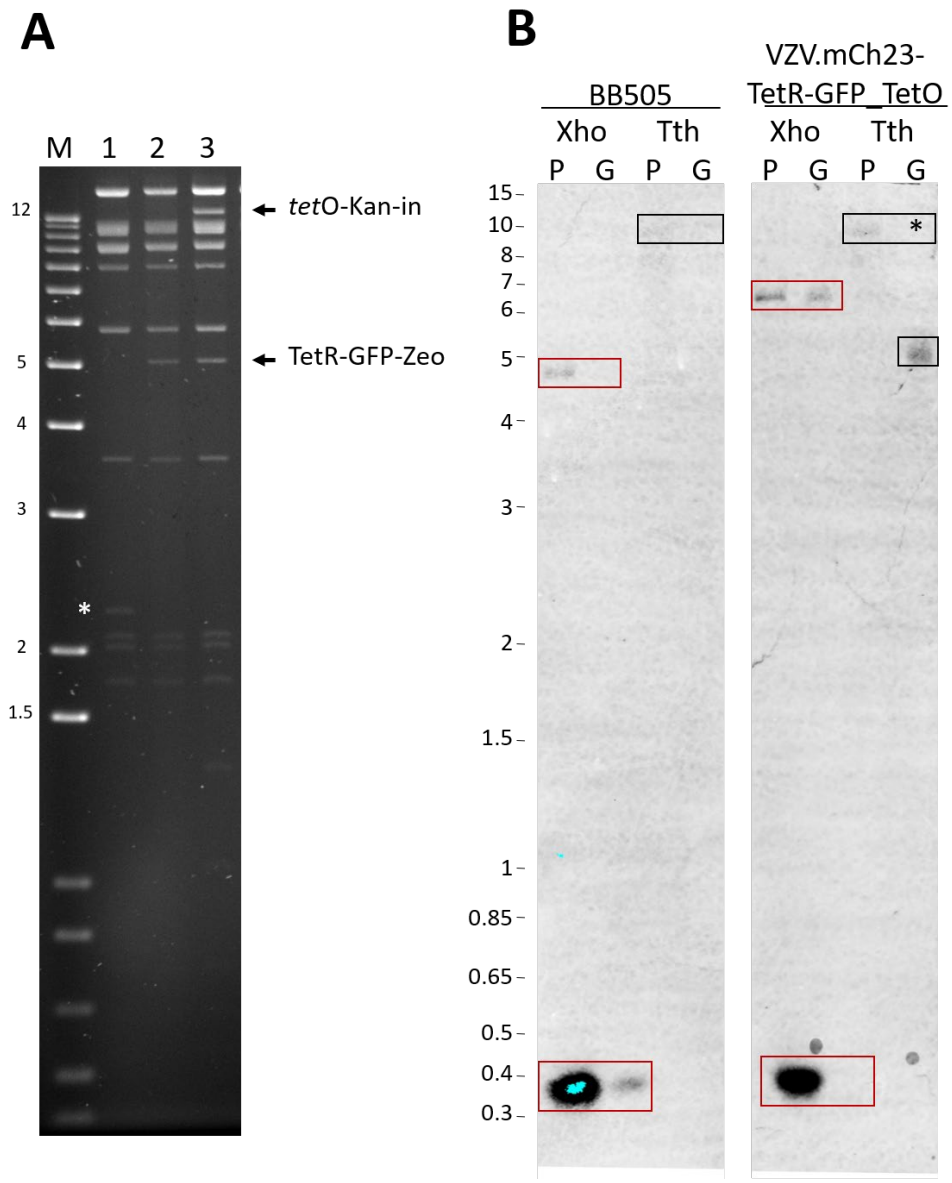

Figure 5. RFLP analysis and Southern blot of new dual-expression BAC DNA.

(A) BAC DNAs were digested with BglII restriction enzyme and separated on a 0.8% agarose gel followed by staining with ethidium bromide (EtBr). Lane M contains the molecular weight standards, with the numbers to the left representing DNA size in kilobases (kb). Lane 1 represents the parental BAC containing mCherry-ORF23. Lane 2 is the parent with the recombined TetR-GFP-Zeo fragment. The parental band just above 2kb (marked by a white asterisk) is shifted up to about 5kb with the addition of TetR-GFP-Zeo. Lane 3 is mCherry-ORF23_TetR-GFP-Zeo with the *tet*O-Kan-in cassette inserted (presence of 12kb fragment). (B) Southern blot of parental plasmid, BAC DNA and gDNAs. Plasmid/BAC DNAs are represented by P and gDNAs are represented by G. The red boxes indicate the correct, expected XhoI fragments except that there were no 347bp fragments in the viral DNA. The asterisk indicated the expected size of the viral DNA Tth111I fragment that was reduced in the generation of the virus.

5.1.2 Aim 1B: Labeling of VZV genomes with click chemistry modifiable nucleotides

Incorporation of EdU allows visualization of viral genomes by fluorescence microscopy.

Another alternative method to FiSH we wanted to investigate was click-labeling of VZV-infected cell viral genomes labeled with EdU. During DNA replication, DNA polymerase incorporates the thymidine analog EdU, which contains a small alkyne modification that allows the chemical addition of an azide fluorophore by a copper catalyst. The copper-catalyzed reaction itself is toxic to cells due to the formation of reactive oxygen species (ROS) [51], so this method requires fixation before click-labeling. There are copper-free systems available for use in live cells, but currently they are only for the labeling of proteins and not nucleic acids. We initially encountered some issues with this method using the standard Click-iT® Edu Imaging Kit (Life Technologies) because even with fixation, the ROS generated during copper-catalyzed labeling reaction denatures GFP and thus diminishes its fluorescent signal [52]. We then used a newer version of the imaging kit (Click-iT® Plus Edu Imaging Kit) which does not affect GFP signal. Our approach was to infect cells with EdU-labeled virus stocks and fix cells at various timepoints to visualize transfer of EdU-labeled genomes into new cells.

Uninfected MRC5 cells were seeded onto 2-well glass chamber slides. The following day the cells were infected with 250 pfu of VZV.GFP-ORF23 labeled with EdU. In a separate chamber the same infection was performed in the presence of phosphonoacetic acid (PAA), which inhibits viral DNA polymerase and thus synthesis of viral DNA [53]. Under these conditions with PAA, we would expect to see GFP-ORF23 only in the input cells because *de novo* infection can only progress up until DNA synthesis. IE62 is made early in infection and thus is made even in the absence of DNA synthesis, so cells that express the EdU-555 and IE62 are newly infected cells. The cells were fixed at 24 hpi. Following fixation of the samples and click-labeling of incorporated

EdU, the cells were stained with an antibody to the VZV IE62 protein and nuclei were counterstained with DAPI and analyzed by immunofluorescence.

Untreated, newly infected cells showed general nuclear, as well as some subnuclear, labeling of DNA with EdU-555 as well as viral IE (IE62) and L (ORF23) proteins (Figure 6A). The arrow indicates a newly infected cell that is adjacent to what we presume to be an input cell that is positive for GFP-ORF23, EdU-555, and IE62. At this timepoint, we would expect to see *de novo* infections that are positive for EdU and the IE62 protein. The lack of GFP-ORF23 in the indicated cell suggests that the protein has not yet been expressed in the newly infected cell. We also observed what we presume to be a third round of infection. That is, a cell that is expressing only IE62 adjacent to a cell in which GFP-ORF23, EdU-555, and IE62 are all expressed suggests that these infections have lost the EdU label following multiple rounds of DNA replication (Figure 6B, yellow arrows). PAA-treated, infected cells displayed punctate EdU-555 signal and positive staining for IE62, but not ORF23 (which is only made following DNA synthesis), suggesting that we are observing *de novo* infection of a new cell and not an infecting cell from the inoculum (Figure 6C). The presence of PAA allows for direct transfer of virus from the infecting cell to an uninfected cell, but will not produce new virus beyond this due to the inhibition of viral DNA polymerase [23].

This data supports click chemistry detection of EdU-labeled VZV genomes as an alternative method to FiSH in productive infections in standard cell culture. Ongoing studies will assess this method in both lytic and latent infections in neuron cultures.

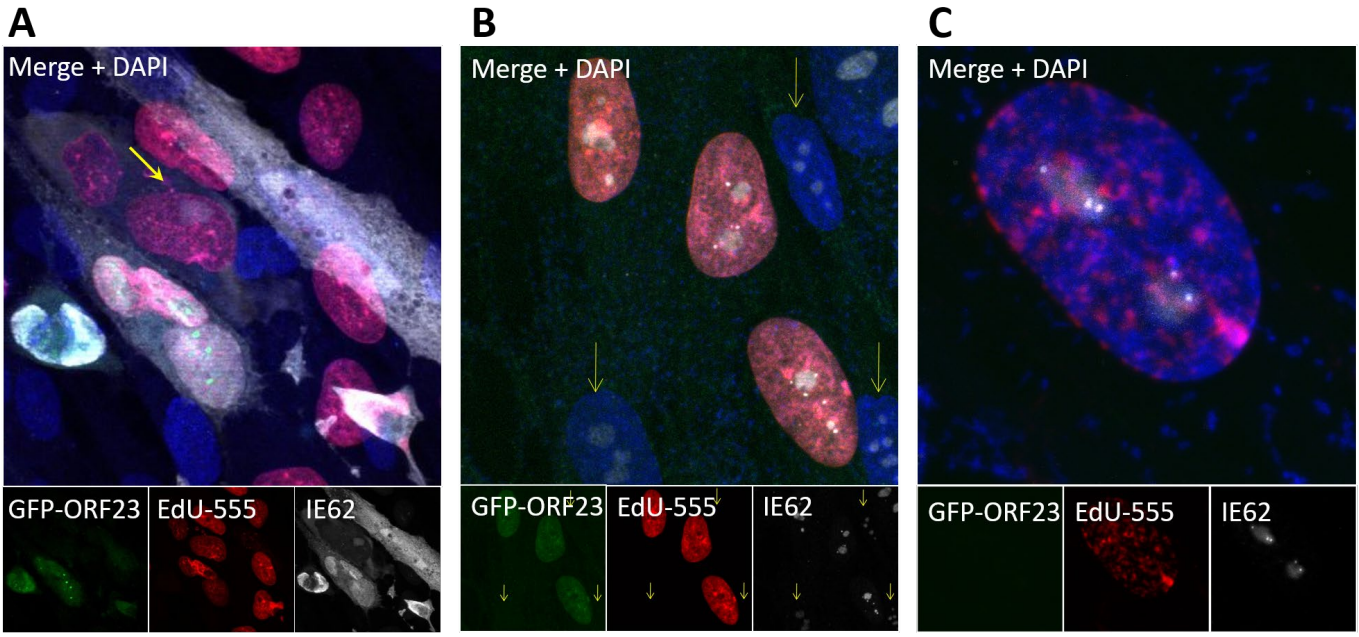

Figure 6. MRC5 cells infected with VZV.GFP-ORF23 labeled with EdU.

MRC5 cells infected with EdU-incorporated VZV-GFP-ORF23 were fixed at 24 hpi. EdU was labeled with click-chemistry and cells were stained for IE62 and nuclei counterstained with DAPI. (A) Cells lacking GFP signal but with positive staining for EdU and IE62 indicates a newly infected cell. Images taken with 40X oil-immersion objective. (B) Cells expressing only VZV IE62 adjacent to cells expressing GFP-ORF23, EdU555, and IE62 suggests infection beyond initial viral replication. (C) Cells were pre-treated with PAA for 2 hours prior to infection and maintained throughout. This magnified nucleus shows a newly infected cell that lacks the late protein GFP-ORF23 but positive for the IE62 protein and EdU label as small puncta, suggesting the virus is sequestered in replication compartments.

5.2 Aim 2: Modeling Viral Latency and Reactivation Using Alternative Systems to hESC-Derived Neurons

VZV causes several diseases involving the CNS, including meningitis, acute disseminated encephalomyelitis (ADEM), vasculopathies and increased risk of stroke [54], all of which underscore the relevancy of using the CNS-derived LUHMES cell line in our studies. LUHMES cells remain proliferative through tetracycline-regulated (Tet-off) constitutive *v-myc* expression [55]. The *v-myc* promoter can be switched off upon the addition of tetracycline (or its synthetic

derivative doxycycline), dibutyryl-cyclic AMP (db-cAMP), and glial cell-derived neurotrophic factor (GDNF) to the media. At this stage the cells stop proliferating and begin to differentiate into post-mitotic neurons [56]. Before assessing permissiveness of LUHMES to VZV infection, we first characterized differentiated LUHMES neurons by immunofluorescence analysis. IF images revealed positive staining for beta-III (βIII) tubulin (a marker for differentiated neurons) and, surprisingly, the presence of the mature peripheral sensory neuron markers peripherin and Brn3a in differentiated LUHMES (Figure 7). While peripherin is expressed primarily in sensory neurons of the peripheral nervous system (PNS), it is also expressed in some neurons of the central nervous system (CNS) [57].

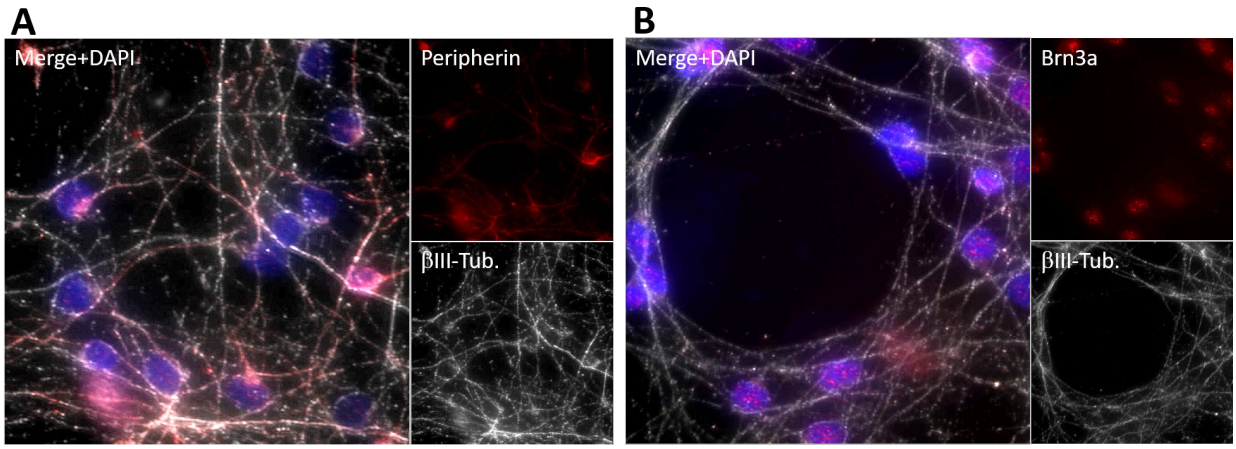

Figure 7. Differentiated LUHMES cells express markers for mature sensory neurons.

LUHMES cells were terminally differentiated for 10 days before being fixed with 4% paraformaldehyde and stained with antibodies to beta-III tubulin (A and B), peripherin (A), Brn3a (B), and the nuclear counterstain DAPI (A and B).

5.2.1 Aim 2A: Establishing permissiveness of LUHMES cells to VZV infection

Both undifferentiated and differentiated LUHMES cells are permissive for VZV lytic infection.

Before assessing the viability of using LUHMES neurons as a model for VZV latency and reactivation studies, we first needed to establish that these cells can support a lytic VZV infection. We first evaluated undifferentiated LUHMES cells for viral spread by infecting cell colonies with a cell-free preparation of the fluorescent reporter virus VZV.GFP-ORF23. Phase-contrast and fluorescence live-cell images were captured from 24 hpi until 8 dpi (Figure 8A). The spread of fluorescence from the initial foci seen at 24 hpi is indicative of lytic viral replication.

Next, we differentiated LUHMES cells into post-mitotic neurons for 7 days. Neurons were infected with cell-free VZV.GFP-ORF23 and phase-contrast and fluorescence live-cell images were captured from 24 hpi until 8 dpi (Figure 8B). Again, the spread of fluorescence in the non-dividing neurons indicates a lytic viral infection.

In a separate experiment, LUHMES cells were differentiated for 49 days before infection with a cell-free preparation of VZV. At 6 dpi, the neurons were fixed and stained for the viral IE62 protein and βIII tubulin. Many neurons were positive for both markers (Figure 9).

Together, these data provide evidence that LUHMES cells and neurons can support a productive VZV lytic infection with cell-free VZV.

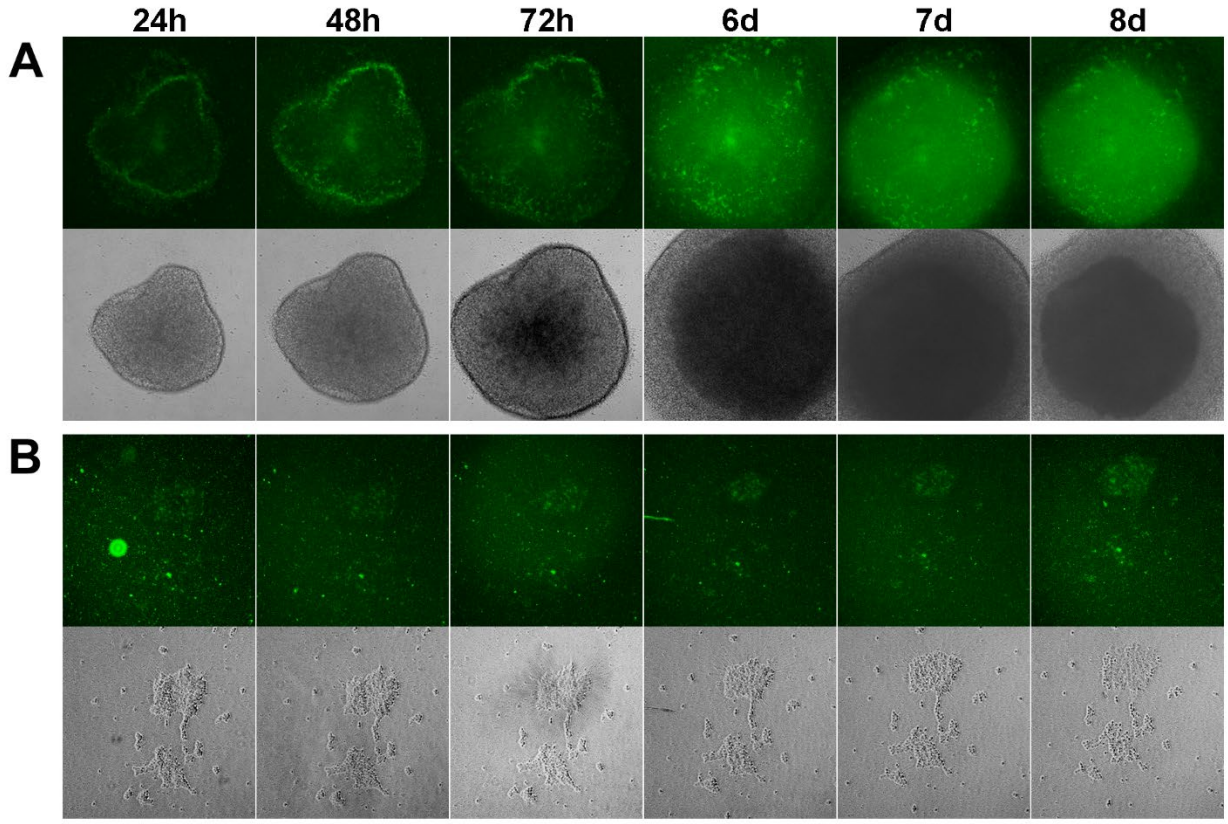

Figure 8. Both undifferentiated and differentiated LUHMES cells support a lytic VZV infection.

Undifferentiated colonies of LUHMES cells (A) and post-mitotic LUHMES neurons (B) were infected with cell-free VZV.GFP-ORF23 and imaged every 24 hours until 8 dpi. Images taken at 10X magnification.

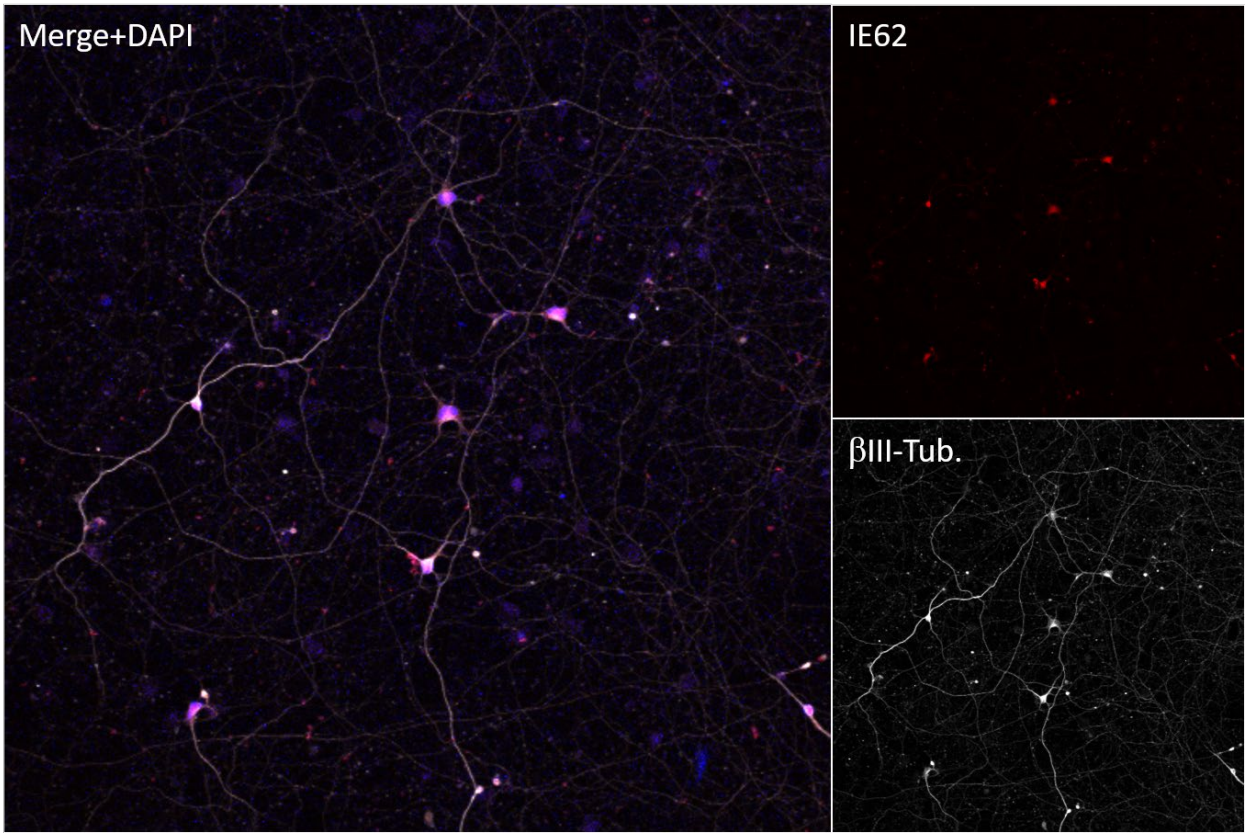

Figure 9. LUHMES neurons are permissive for VZV infection.

LUHMES cells were terminally differentiated for 49 days and then infected with cell-free VZV. At 6 dpi, the cells were fixed with 4% paraformaldehyde and stained with antibodies to VZV IE62, β-III tubulin, and DAPI. Images taken at 20X.

5.2.2 Aim 2B: Establishment of latency in LUHMES neurons

LUHMES neurons can host a reactivatable latent VZV state.

To assess the viability of using LUHMES neurons to model VZV latency and reactivation, LUHMES cells were plated on 2 coated 12-well dishes and allowed to proliferate overnight. The following day, the media was changed to differentiation medium and the cells were maintained in this medium for 7 days, with media changes every other day. Four wells of one plate were left uninfected, and the remaining neurons were infected with a cell-free preparation of VZV-pOka

diluted 1:10 in culture medium both in the absence and presence of the antiviral brivudine (BVDU). Virus was adsorbed for 2 hours at 37ºC, washed with PBS, and culture medium was maintained as follows: 4 wells uninfected, standard medium; 4 wells pOka, standard medium; 16 wells pOka in the presence of 2 μM BVDU (pOka+BVDU) (Figure 10). Media was changed every third day until 7dpi, at which point Plate 1 (uninfected wells, pOka wells, 4 wells of pOka+BVDU) was harvested for DNA and RNA. At 8 dpi BVDU was removed from the media in Plate 2 and changed to differentiation medium plus the following: 4 wells no addition; 4 wells add 4μM sodium butyrate (NaB); 4 wells add 10 μM PI3K-Inhibitor (PI3K-i) LY294002. Media conditions were maintained for an additional 7 days, with media changes every third day until 14 dpi, at which point cells were harvested for DNA and RNA. Identical experiments were set up with hESC-derived neurons as positive controls.

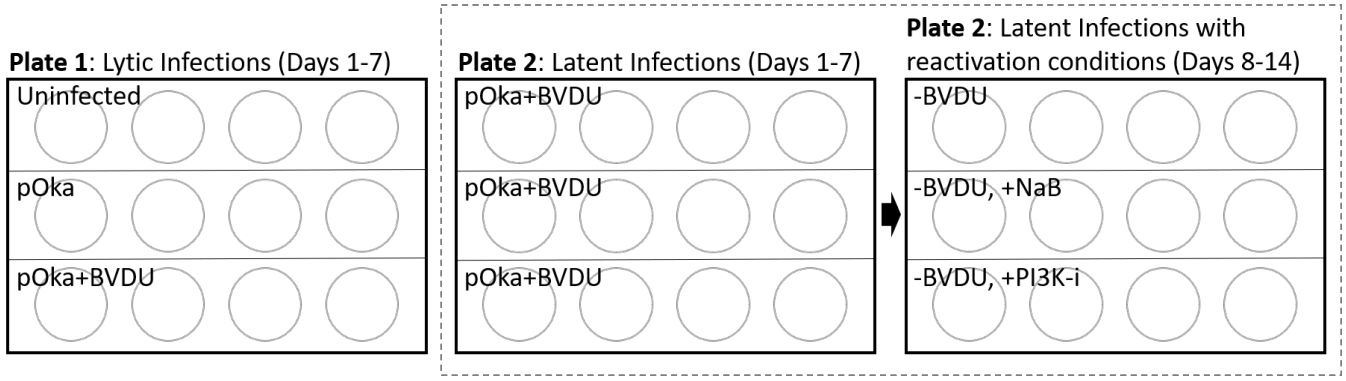

Figure 10. Plate setup for lytic and latent infection experiments.

Media conditions and infections are described in text. Plate 1 was harvested for DNA and RNA at 7 dpi. At 8 dpi, media was changed on plate 2 (dashed outline) to the appropriate conditions indicated on the far right diagram. At 14 dpi, plate 2 was harvested for DNA and RNA.

Real-time qPCR was performed on 100 ng of each DNA sample. The ratios of absolute copy numbers of the terminal region to ORF49 are shown in Figure 11. Values greater than or equal to 1 indicate a latent infection because there are more circular genomes present than linear genomes. Values closer to 0 indicate that there are more linear genomes present than there are

circular, signifying a lytic infection. We expected to see no amplification from the uninfected cells from either primer set as they are virus specific. We expected to see ratios closer to 0 for the infected-only cells because the virus is actively replicating. For the infections in the presence of BVDU, we expected to see ratios ≥ 1 because the genomes should be circularized due to the prevention of viral replication. We expected to see values closer to 0 in the samples where BVDU was removed and reactivation was stimulated by the addition of NaB or PI3K-i. The data obtained from the LUHMES experiments (Figure 11B) met these expectations and mirrored results seen with hESC-derived neurons (Figured 11A). This provided evidence that a latent infection can be established in LUHMES-derived neurons that can be experimentally reactivated to produce a lytic infection.

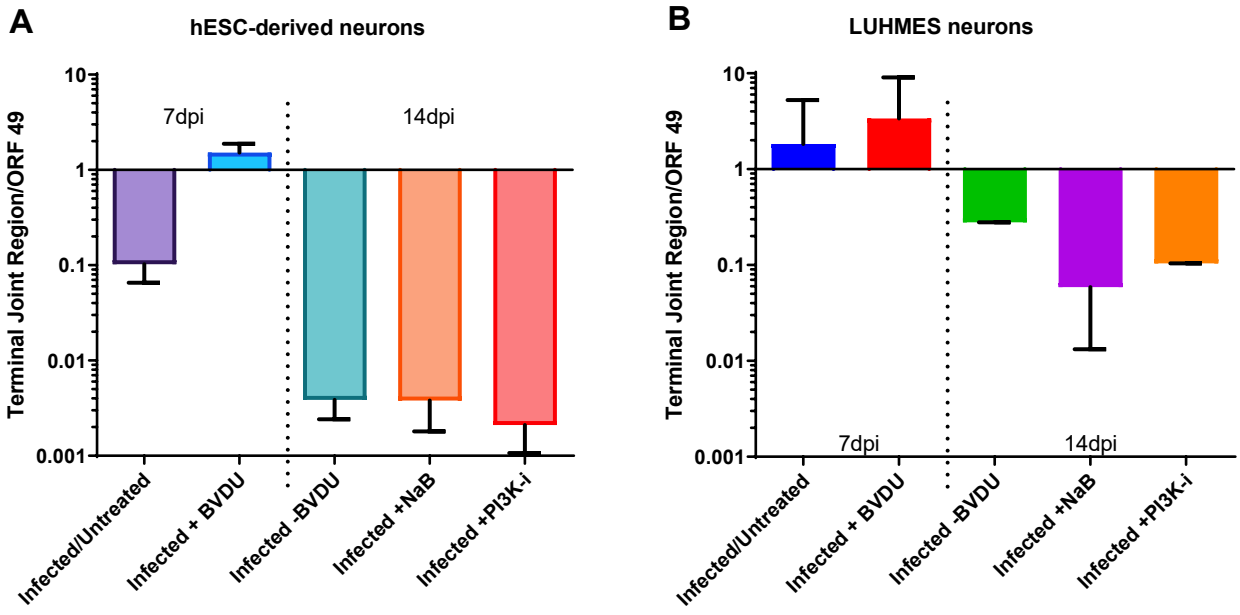

Figure 11. Ratios of absolute copy numbers of terminal joint region to ORF49.

Absolute copy numbers were calculated for each sample amplifying from the terminal joint region (TR) and from the internal ORF49. Panel A contains data from hESC-derived neurons and panel B contains data from differentiated LUHMES neurons. The ratio of TR/ORF49 for each condition was calculated and graphed. Data shown is from 2 independent experiments, each with 4 replicates per condition for a total of N=8 replicates per condition. There was no amplification from the uninfected samples and were thus omitted for simplicity.

LUHMES neurons generate extensive neurites that can be isolated using microfluidics devices.

In parallel experiments, both hESC neurons and LUHMES cells were seeded in the Soma chamber of a microfluidics device and allowed to differentiate into neurons and extend neurite processes through the microchannels for 21 days. Mitotically inhibited, cell-associated EdU-labeled-VZV.GFP-ORF23 was then added to the axon chamber of the device and incubated for 14 days. The cells were then analyzed by immunofluorescence microscopy following click-chemistry labeling of the neuron soma. We were able to detect few EdU-specific foci in the nuclei of some hESC neurons (Figure 12A) and LUHMES neurons (Figure 12B). While latent infections should have theoretically been established at 14 dpi, the presence of the viral proteins ORF23 and IE62 indicate otherwise. They should only be expressed during a lytic infection. Regardless, this data further supports utilizing LUHMES neurons in axon-isolation infections. Ongoing experiments will address the appropriate timeframe at which VZV establishes a latent infection in the absence of antivirals. We will also utilize BVDU to establish latent infections in upcoming experiments, and we will then assess whether we can reactivate these latent infections to induce lytic replication to generate infectious virus.

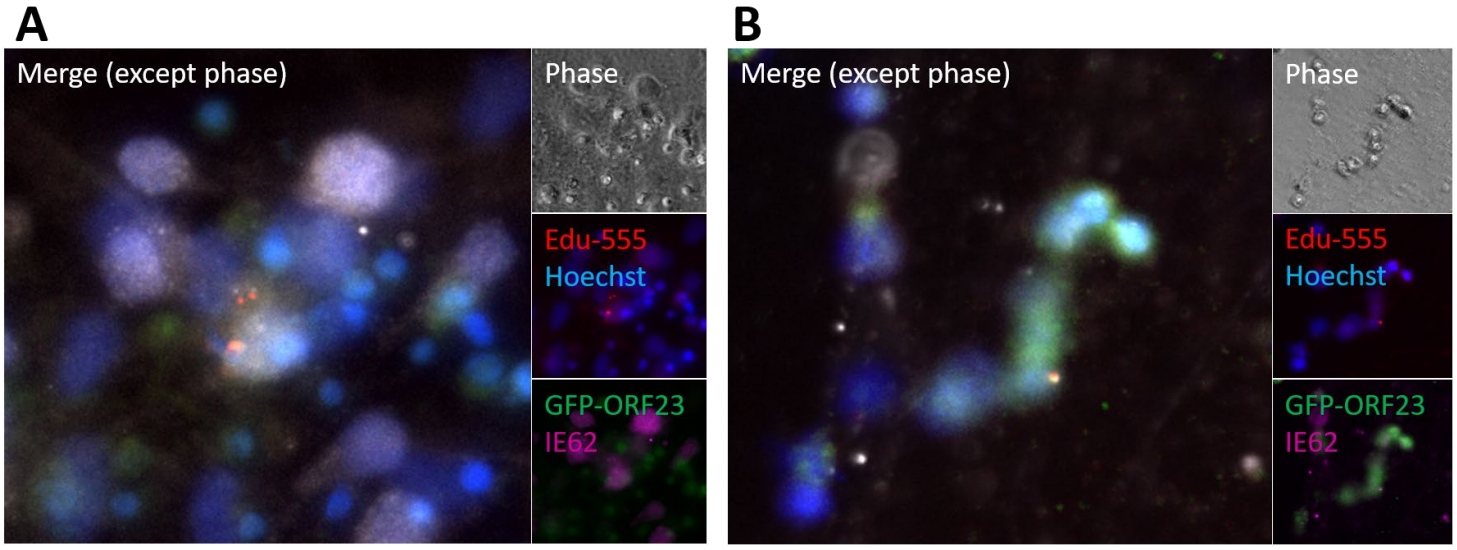

Figure 12. EdU-labeled VZV genomes present in neuronal soma following axonal infection.

(A) HESC neurons and LUHMES neurons (B) were seeded in the Soma chambers of microfluidics devices and differentiated for 21 days. The axon chambers were infected with cell-associated mitotically inhibited EdU-labeled VZV-GFP23. The Soma chambers were fixed at 14 dpi, followed by click labeling, immunofluorescence staining for VZV IE62, and nuclear counterstain with Hoechst 33342. In the two-color panels, IE62 is magenta, however to allow for distinction between magenta and red, IE62 is pseudocolored gray in the four color merged images. Images were taken at 40X magnification with an air objective.

6.0 Discussion

While our attempts to label VZV genomes in live cells utilizing VZV co-expressing both the *tet*O genetic elements and the TetR-GFP protein were not as successful as we had hoped, this fluorescent repressor-operator system of tagging viral genomes has been shown in adenovirus [58] and other herpesviruses ([43] and B. Kaufer, personal communication). Both prokaryotic and eukaryotic cells possess mechanisms to eliminate repeated DNA sequences, which may explain the difficulties we experienced in generating the *tet*O/TetR-GFP construct. Other researchers have circumvented this repair mechanism by inserting unique spacer sequences between multimers of the *tet*O elements, thereby reducing the chances of the repeated sequences being eliminated from the genome [59]. This approach may improve the system in our hands in the future. However, we will proceed with the caveat that there still exits the potential for chromosome rearrangements between the repetitive homologous sequences [60]. In latency experiments, it is possible that the TetR-GFP protein may not be able to access the *tet*O elements due to chromatinization of the genome. Another possible locus in the VZV genome for inserting the *tet*O cassette would be in the ORF61-62 region. It is in this region that the VZV VLT was identified [34], suggesting that perhaps this region is not silenced by chromatin, or at least not to a large extent. Although the Southern blot results suggest that about half of the repeat elements were deleted, perhaps there are enough genetic elements remaining to pursue this method further in ongoing neuron latent infections. It might also be more beneficial to place the TetR-GFP expression under an inducible promoter, such as the tetracycline promoter, so that the TetR-GFP protein is only made under specified conditions.

Labeling of HSV genomes with ethynyl-modified nucleosides coupled with click-chemistry has proven to be an invaluable tool to track viral genomes as well as identify proteins associated with the viral genome [61, 62]. In our hands, this method has allowed us to visualize viral genomes during lytic, and possibly latent, VZV infections. The presence of viral proteins in neurons that were EdU-positive indicates that we may not have established a latent infection, even after the assumed 14-day induction of latency. Further optimization is necessary to continue to explore the latent state in more detail. If we can achieve this, we would also like to develop studies with both hESC-derived and LUHMES neurons in which we can identify cells harboring latent viral genomes and isolate them through laser-capture microdissection. The goal of these studies would be to analyze the host and viral mRNA transcripts to better understand the cellular and/or viral factors involved in establishing and maintaining latency, and the requirements for inducing reactivation. It is possible that we can utilize isolation of proteins on nascent DNA (iPOND) in conjunction with EdU/click-chemistry to demonstrate these interactions without the need for laser capture microdissection.

The field of VZV latency and reactivation continues to be of great interest to researchers around the world. While an *in vivo* model system would greatly substantiate *in vitro* data, there is no viable option that can adequately model all aspects of the VZV life cycle and disease. While the hESC-derived neuron model system has allowed us to successfully model the lytic cycle of VZV infection as well as a reactivatable latent infection, reactivation in these neurons is inefficient. LUHMES cells have been widely used for neurotoxicity studies [63] and to study neurodegenerative diseases, such as Parkinson's disease [64]. In addition, a recent study has demonstrated that LUHMES neurons can support a latent HSV-1 infection that can be reactivated [44], and as an extension possibly other neurotropic viruses. This evidence validates exploring the

LUHMES neuron system further for studying VZV infections. In this work, we have successfully demonstrated an alternative to the hESC-neuron model system with the ability to study both the lytic and latent cycle of VZV infection and reactivation. While the results of the experiments shown here demonstrate that LUHMES can be highly permissive to lytic replication, the results of reactivatable latent infection are still preliminary. We plan to perform more extensive qPCR analyses to further solidify this model for latency/reactivation studies. We have obtained RNA from the same samples in which we obtained the gDNA used in the qPCR studies. Ideally, these can be reverse transcribed into cDNA and analyzed for kinetic class transcripts as well as the VZV VLT, which would allow for the differentiation between and characterization of lytic and latent infections.

The LUHMES neuron system is a more attractive platform for studying VZV for several reasons. Initiating studies with hESCs is an expensive undertaking which entails obtaining approval to work with them. The purchase price of one vial of hESCs is about 3-4 times as much as common cell culture lines and they are only available from select vendors. LUHMES cells, however, are commercially available without restriction and can be propagated rather easily. The specialized training that is required to culture hESCs took several months to develop in our lab, and some level of spontaneous differentiation of the cultures remains unavoidable. Expansion of co-cultures to generate large numbers of hESC-neurons is an incredibly tedious and time-consuming process. On the other hand, scaling up of LUHMES cells is relatively simple as they are maintained using standard cell culturing methods and proliferate rapidly. Biochemical and molecular assays which require high cell numbers, including assessment of chromatin changes, may be obtainable with the ease of scalability of LUHMES cells. The timeline for differentiation into mature neurons is also more rapid with the LUHMES model (5-7 days vs. 14-28 days for

hESCs). They are also cultured as single cells which makes the differentiated neurons easier to image by microscopy, unlike the difficulties faced when imaging large dense 3D spheroid structures of hESC-derived neurospheres. Previous reports have rarely shown survival of LUHMES neurons beyond 21 days, while mature hESC-derived neurons have been shown to survive for up to 5 months in culture [65]. However, in this body of work, we have found LUHMES neurons can remain viable in culture for at least 55 days. Long-term latency studies in these neurons are the next logical step for future experiments.

This system may not be a direct substitution for the hESC-derived neuron model in all cases, as there are many unanswered questions with LUHMES neurons. Can infected LUHMES neurons generate the VZV VLT RNA? Do LUHMES neurons demonstrate comparable VZV axonal transport efficiencies as hESC neurons? The neuronal phenotypes of differentiated LUHMES neurons needs to be further evaluated as well. Thus far we have qualitatively identified the presence of peripherin and Brn3a, both markers of peripheral sensory neurons, in LUHMES neurons, but the number of neurons expressing these markers have not yet been quantified. In hESC-derived neurons, it is estimated that only around 10% of neurons are peripherin and Brn3a positive [19]. In both systems, there are very few glial fibrillary acidic protein (GFAP) positive glial cells, suggesting that our differentiation protocols are perhaps selectively enhancing survival of non-dividing neuronal cells over proliferating non-neuronal cells. Though these different neurons represent two different branches of the nervous system, the differentiation phenotypes are quite similar. This is also pertinent to the fact that VZV can infect ganglia in both the PNS and CNS. An interesting direction for future work would be to extend these LUHMES neuron studies in a more physiologically relevant system involving myelinated axons. It has been demonstrated that hESCs can be differentiated into Schwann cells that, when co-cultured with isolated axons,

form a myelin sheath around the axons [66]. Schwann cells play an important role in nerve development and regeneration, presentation of antigens to T-lymphocytes, and are also permissive to VZV infection [67]. Utilizing our microfluidics devices in the generation of myelinated axons *in vitro* may help to advance the knowledge of VZV immunobiology without the need for expensive SCID-hu mouse experiments.

Further experiments are planned to explore reactivation of latent VZV resulting in production of infectious virus. This approach will involve using the microfluidics chamber system to isolate the axons from the soma in LUHMES and hESC neurons. The neuron soma will be infected with fluorescent cell-associated VZV or cell-free VZV in the presence of brivudine so that lytic replication cannot occur in the neuronal nuclei. Neurons will be maintained under these media conditions for 14 days, at which point uninfected RPE cells will be seeded in the axon chamber so that the cells will make direct contact with the axons. Brivudine will be removed from the soma media and either NaB or PI3K-i, or both, will be applied to the soma compartment. This should release the repressed viral genome and allow for lytic replication. If infectious virus is generated, it should travel by anterograde axonal transport to the axon chamber where the virus will infect the RPE cells. Presence of fluorescent RPEs in the axon chamber would indicate successful, true reactivation. Success in this area would open the door for the electrophysiological study of soma and/or axon fusion. Our lab is also investigating a method that may induce immediate latent infections in neurons. This method employs a degron system in which we exploit the destabilizing domain of the *E. coli* dihydrofolate reductase (DHFR). In this method, a protein that is fused to DHFR becomes unstable, signaling the ubiquitin-dependent proteasomal pathway (UPP) for poly-ubiquitination of the protein fusion and trafficking to the proteasome for degradation [68]. However, in the presence of trimethoprim (TMP), a small-molecule ligand, the

destabilizing domain is stabilized, preventing signaling of the UPP and the resultant proteasomal degradation. Of importance, the stabilizing action of TMP is dose-dependent, fully reversible, generally non-cytotoxic, and has a much greater affinity for bacterial DHFR over eukaryotic DHFR. Our approach would be to tag a VZV protein that is essential for viral replication. We have developed a VZV in which the essential gene product of ORF4 is fused with DHFR and is tightly regulated by TMP (Ben Warner, unpublished data). Utilizing our microfluidics devices, we can infect neuronal axons with this virus in the absence of TMP. The virus will still be able to infect the axons and travel to the soma because functional ORF4 will still be packaged in the virion tegument, but lytic replication should not occur since any *de novo* ORF4 protein that is made will be immediately degraded. In theory the virus should immediately establish a latent infection and should be reactivatable by induction with NaB and/or PI3K-I plus the addition of TMP to allow ORF4 to be stably expressed again. There are other essential viral proteins we can explore with this method and we can potentially combine the DHFR method with our viral genome tagging strategies.

Shingles is still a relevant public health concern in our modern society despite the advent of 2 different vaccines to prevent the disease from occurring. There are also limited model systems in which researchers can employ to study the full infection and disease caused by VZV. Our goal is to develop a more physiologically relevant system in which to study the latent infection and reactivation process so that we may help to advance insight into not only the VZV research field but other neurotropic virus research as well.

Appendix: Publications

1. McSharry, B.P., Samer C., McWilliam H.E.G., Ashley C.L., **Yee M.B.**, Steain M., Liu L., Fairlie D.P., Kinchington P.R., McCluskey J., Abendroth A., Villadangos J.A., Rossjohn J., Slobedman B., *Virus-Mediated Suppression of the Antigen Presentation Molecule MR1.* Cell Rep, 2020. **30**(9): p. 2948-2962 e4.

2. Kramer, P.R., Stinson C., Umorin M., Deng M., Rao M., Bellinger L., **Yee M.B.**, Kinchington P.R., *Aromatase Derived Estradiol Within the Thalamus Modulates Pain Induced by Varicella Zoster Virus.* Front Integr Neurosci, 2018. **12**: p. 46.

3. Stinson, C., Deng M., **Yee M.B.**, Bellinger L.L., Kinchington P.R., Kramer P.R., *Sex differences underlying orofacial varicella zoster associated pain in rats.* BMC Neurol, 2017. **17**(1): p. 95.

4. Kramer, P.R., Strand J., Stinson C., Bellinger L.L., Kinchington P.R., **Yee M.B.**, Umorin M., Peng Y.B., *Role for the Ventral Posterior Medial/Posterior Lateral Thalamus and Anterior Cingulate Cortex in Affective/Motivation Pain Induced by Varicella Zoster Virus.* Front Integr Neurosci, 2017. **11**: p. 27.

5. Kramer, P.R., Stinson C., Umorin M., Deng M., Rao M., Bellinger L., **Yee M.B.**, Kinchington P.R., *Lateral thalamic control of nociceptive response after whisker pad injection of varicella zoster virus.* Neuroscience, 2017. **356**: p. 207-216.

6. McNulty, J., D'Aiuto L., Zhi Y., McClain L., Zepeda-Velázquez C., Ler S., Jenkins H.A., **Yee M.B.**, Piazza P., Yolken R.H., Kinchington P.R., and Nimgaonkar V.L., *iPSC Neuronal Assay Identifies Amaryllidaceae Pharmacophore with Multiple Effects against Herpesvirus Infections.* ACS Med Chem Lett, 2016. **7**(1): p. 46-50.

7. McClain, L., Zhi Y., Cheng H., Ghosh A., Piazza P., **Yee M.B.**, Kumar S., Milosevic J., Bloom D.C., Arav-Boger R., Kinchington P.R., Yolken R., Nimgaonkar V., D'Aiuto L., *Broad-spectrum non-nucleoside inhibitors of human herpesviruses.* Antiviral Res, 2015. **121**: p. 16-23.

8. Guedon, J.M., **Yee M.B.**, Zhang M., Harvey S.A., Goins W.F., Kinchington P.R., *Neuronal changes induced by Varicella Zoster Virus in a rat model of postherpetic neuralgia.* Virology, 2015. **482**: p. 167-80.

9. Grigoryan, S., **Yee M.B.**, Glick Y., Gerber D., Kepten E., Garini Y., Yang I.H., Kinchington P.R., Goldstein R.S., *Direct transfer of viral and cellular proteins from varicella-zoster virus-infected non-neuronal cells to human axons.* PLoS One, 2015. **10**(5): p. e0126081.

10. Sloutskin, A., **Yee M.B.**, Kinchington P.R., Goldstein R.S., *Varicella-zoster virus and herpes simplex virus 1 can infect and replicate in the same neurons whether co- or superinfected.* J Virol, 2014. **88**(9): p. 5079-86.

11. Jones, M., Dry I.R., Frampton D., Singh M., Kanda R.K., **Yee M.B.**, Kellam P., Hollinshead M., Kinchington P.R., O'Toole E.A., Breuer J., *RNA-seq analysis of host and viral gene expression highlights interaction between varicella zoster virus and keratinocyte differentiation.* PLoS Pathog, 2014. **10**(1): p. e1003896.

12. Grigoryan, S., Kinchington P.R., Yang I.H., Selariu A., Zhu H., **Yee M.**, Goldstein R.S., *Retrograde axonal transport of VZV: kinetic studies in hESC-derived neurons.* J Neurovirol, 2012. **18**(6): p. 462-70.

13. Dukhovny, A., Sloutskin A., Markus A., **Yee M.B.**, Kinchington P.R., Goldstein R.S., *Varicella-zoster virus infects human embryonic stem cell-derived neurons and neurospheres but not pluripotent embryonic stem cells or early progenitors.* J Virol, 2012. **86**(6): p. 3211-8.

14. Markus, A., Grigoryan S., Sloutskin A., **Yee M.B.**, Zhu H., Yang I.H., Thakor N.V., Sarid R., Kinchington P.R., Goldstein R.S., *Varicella-zoster virus (VZV) infection of neurons derived from human embryonic stem cells: direct demonstration of axonal infection, transport of VZV, and productive neuronal infection.* J Virol, 2011. **85**(13): p. 6220-33.

15. Erazo, A., **Yee M.B.**, Banfield B.W., Kinchington P.R., *The alphaherpesvirus US3/ORF66 protein kinases direct phosphorylation of the nuclear matrix protein matrin 3.* J Virol, 2011. **85**(1): p. 568-81.

16. Ramachandran, S., Davoli K.A., **Yee M.B.**, Hendricks R.L., Kinchington P.R., *Delaying the expression of herpes simplex virus type 1 glycoprotein B (gB) to a true late gene alters neurovirulence and inhibits the gB-CD8+ T-cell response in the trigeminal ganglion.* J Virol, 2010. **84**(17): p. 8811-20.

17. Knickelbein, J.E., Khanna K.M., **Yee M.B.**, Baty C.J., Kinchington P.R., Hendricks R.L., *Noncytotoxic lytic granule-mediated CD8+ T cell inhibition of HSV-1 reactivation from neuronal latency.* Science, 2008. **322**(5899): p. 268-71.

18. Erazo, A., **Yee M.B.**, Osterrieder N., Kinchington P.R., *Varicella-zoster virus open reading frame 66 protein kinase is required for efficient viral growth in primary human corneal stromal fibroblast cells.* J Virol, 2008. **82**(15): p. 7653-65.

19. Eisfeld, A.J., **Yee M.B.**, Erazo A., Abendroth A., Kinchington P.R., *Downregulation of class I major histocompatibility complex surface expression by varicella-zoster virus involves open reading frame 66 protein kinase-dependent and -independent mechanisms.* J Virol, 2007. **81**(17): p. 9034-49.

Bibliography

1. Pergam, S.A., A.P. Limaye, and A.S.T.I.D.C.o. Practice, *Varicella zoster virus (VZV) in solid organ transplant recipients.* Am J Transplant, 2009. **9 Suppl 4**: p. S108-15.
2. Mueller, N.H., et al., *Varicella zoster virus infection: clinical features, molecular pathogenesis of disease, and latency.* Neurologic clinics, 2008. **26**(3): p. 675-viii.
3. Reichelt, M., L. Zerboni, and A.M. Arvin, *Mechanisms of varicella-zoster virus neuropathogenesis in human dorsal root ganglia.* J Virol, 2008. **82**(8): p. 3971-83.
4. Gershon, A.A., et al., *Latency of varicella zoster virus in dorsal root, cranial, and enteric ganglia in vaccinated children.* Trans Am Clin Climatol Assoc, 2012. **123**: p. 17-33; discussion 33-5.
5. Nagel, M.A., et al., *Frequency and abundance of alphaherpesvirus DNA in human thoracic sympathetic ganglia.* J Virol, 2014. **88**(14): p. 8189-92.
6. Catron, T. and H.G. Hern, *Herpes zoster ophthalmicus.* West J Emerg Med, 2008. **9**(3): p. 174-6.
7. Marin, M., H.C. Meissner, and J.F. Seward, *Varicella prevention in the United States: a review of successes and challenges.* Pediatrics, 2008. **122**(3): p. e744-51.
8. Keating, G.M., *Shingles (Herpes Zoster) Vaccine (Zostavax((R))): A Review in the Prevention of Herpes Zoster and Postherpetic Neuralgia.* BioDrugs, 2016. **30**(3): p. 243-54.
9. Bharucha, T., D. Ming, and J. Breuer, *A critical appraisal of 'Shingrix', a novel herpes zoster subunit vaccine (HZ/Su or GSK1437173A) for varicella zoster virus.* Hum Vaccin Immunother, 2017. **13**(8): p. 1789-1797.
10. Syed, Y.Y., *Recombinant Zoster Vaccine (Shingrix((R))): A Review in Herpes Zoster.* Drugs Aging, 2018. **35**(12): p. 1031-1040.
11. Straus, S.E., *Overview: the biology of varicella-zoster virus infection.* Ann Neurol, 1994. **35 Suppl**: p. S4-8.
12. Cohen, J.I., *The varicella-zoster virus genome.* Curr Top Microbiol Immunol, 2010. **342**: p. 1-14.
13. Spengler, M., et al., *Interactions among structural proteins of varicella zoster virus.* Arch Virol Suppl, 2001(17): p. 71-9.
14. Laemmle, L., R.S. Goldstein, and P.R. Kinchington, *Modeling Varicella Zoster Virus Persistence and Reactivation - Closer to Resolving a Perplexing Persistent State.* Front Microbiol, 2019. **10**: p. 1634.
15. Markus, A., et al., *An In Vitro Model of Latency and Reactivation of Varicella Zoster Virus in Human Stem Cell-Derived Neurons.* PLOS Pathogens, 2015. **11**(6): p. e1004885.
16. Luxton, G.W., et al., *Targeting of herpesvirus capsid transport in axons is coupled to association with specific sets of tegument proteins.* Proc Natl Acad Sci U S A, 2005. **102**(16): p. 5832-7.
17. Diefenbach, R.J., et al., *Transport and egress of herpes simplex virus in neurons.* Rev Med Virol, 2008. **18**(1): p. 35-51.

18. Antinone, S.E., et al., *The Herpesvirus capsid surface protein, VP26, and the majority of the tegument proteins are dispensable for capsid transport toward the nucleus.* J Virol, 2006. **80**(11): p. 5494-8.
19. Markus, A., et al., *Varicella-zoster virus (VZV) infection of neurons derived from human embryonic stem cells: direct demonstration of axonal infection, transport of VZV, and productive neuronal infection.* J Virol, 2011. **85**(13): p. 6220-33.
20. Bleymehl, K., J. Cinatl, and J. Schmidt-Chanasit, *Phenotypic and genetic characterization of varicella-zoster virus mutants resistant to acyclovir, brivudine and/or foscarnet.* Med Microbiol Immunol, 2011. **200**(3): p. 193-202.
21. Laing, K.J., et al., *Immunobiology of Varicella-Zoster Virus Infection.* J Infect Dis, 2018. **218**(suppl_2): p. S68-S74.
22. Zerboni, L., et al., *Molecular mechanisms of varicella zoster virus pathogenesis.* Nature reviews. Microbiology, 2014. **12**(3): p. 197-210.
23. Cliffe, A.R. and A.C. Wilson, *Restarting Lytic Gene Transcription at the Onset of Herpes Simplex Virus Reactivation.* J Virol, 2017. **91**(2).
24. Walters, M.S., et al., *Hyperphosphorylation of histone deacetylase 2 by alphaherpesvirus US3 kinases.* J Virol, 2010. **84**(19): p. 9666-76.
25. Camarena, V., et al., *Nature and duration of growth factor signaling through receptor tyrosine kinases regulates HSV-1 latency in neurons.* Cell host & microbe, 2010. **8**(4): p. 320-330.
26. Sadaoka, T., et al., *In vitro system using human neurons demonstrates that varicella-zoster vaccine virus is impaired for reactivation, but not latency.* Proc Natl Acad Sci U S A, 2016. **113**(17): p. E2403-12.
27. Carpenter, J.E., E.P. Henderson, and C. Grose, *Enumeration of an extremely high particle-to-PFU ratio for Varicella-zoster virus.* J Virol, 2009. **83**(13): p. 6917-21.
28. Buckingham, E.M., et al., *Exocytosis of Varicella-Zoster Virus Virions Involves a Convergence of Endosomal and Autophagy Pathways.* J Virol, 2016. **90**(19): p. 8673-85.
29. Shiraki, K., et al., *Pathogenetic tropism of varicella-zoster virus to primary human hepatocytes and attenuating tropism of Oka varicella vaccine strain to neonatal dermal fibroblasts.* J Infect Dis, 2003. **188**(12): p. 1875-7.
30. Pomp, O., et al., *PA6-induced human embryonic stem cell-derived neurospheres: a new source of human peripheral sensory neurons and neural crest cells.* Brain Research, 2008. **1230**: p. 50-60.
31. Gowrishankar, K., et al., *Productive varicella-zoster virus infection of cultured intact human ganglia.* J Virol, 2007. **81**(12): p. 6752-6.
32. Hood, C., et al., *Varicella-zoster virus ORF63 inhibits apoptosis of primary human neurons.* J Virol, 2006. **80**(2): p. 1025-31.
33. Steain, M., et al., *Upregulation of CXCL10 in human dorsal root ganglia during experimental and natural varicella-zoster virus infection.* J Virol, 2011. **85**(1): p. 626-31.
34. Depledge, D.P., et al., *A spliced latency-associated VZV transcript maps antisense to the viral transactivator gene 61.* Nat Commun, 2018. **9**(1): p. 1167.
35. Clarke, P., et al., *Configuration of latent varicella-zoster virus DNA.* J Virol, 1995. **69**(12): p. 8151-4.
36. Azarkh, Y., et al., *Human trigeminal ganglionic explants as a model to study alphaherpesvirus reactivation.* J Neurovirol, 2012. **18**(6): p. 456-61.

37. Christensen, J., et al., *Differentiated neuroblastoma cells provide a highly efficient model for studies of productive varicella-zoster virus infection of neuronal cells.* J Virol, 2011. **85**(16): p. 8436-42.
38. Hanani, M., *Satellite glial cells in sensory ganglia: from form to function.* Brain Res Brain Res Rev, 2005. **48**(3): p. 457-76.
39. Zerboni, L., et al., *Varicella-zoster virus infection of human dorsal root ganglia in vivo.* Proc Natl Acad Sci U S A, 2005. **102**(18): p. 6490-5.
40. Johnson, R.W., et al., *Herpes zoster epidemiology, management, and disease and economic burden in Europe: a multidisciplinary perspective.* Ther Adv Vaccines, 2015. **3**(4): p. 109-20.
41. Dooling, K.L., et al., *Recommendations of the Advisory Committee on Immunization Practices for Use of Herpes Zoster Vaccines.* MMWR Morb Mortal Wkly Rep, 2018. **67**(3): p. 103-108.
42. Bertke, A.S., et al., *A5-positive primary sensory neurons are nonpermissive for productive infection with herpes simplex virus 1 in vitro.* J Virol, 2011. **85**(13): p. 6669-77.
43. Sourvinos, G. and R.D. Everett, *Visualization of parental HSV-1 genomes and replication compartments in association with ND10 in live infected cells.* EMBO J, 2002. **21**(18): p. 4989-97.
44. Edwards, T.G. and D.C. Bloom, *Lund Human Mesencephalic (LUHMES) Neuronal Cell Line Supports Herpes Simplex Virus 1 Latency In Vitro.* J Virol, 2019. **93**(6).
45. Tischer, B.K., et al., *Two-step red-mediated recombination for versatile high-efficiency markerless DNA manipulation in Escherichia coli.* Biotechniques, 2006. **40**(2): p. 191-7.
46. Sloutskin, A. and R.S. Goldstein, *Laboratory preparation of Varicella-Zoster Virus: concentration of virus-containing supernatant, use of a debris fraction and magnetofection for consistent cell-free VZV infections.* J Virol Methods, 2014. **206**: p. 128-32.
47. Tischer, B.K., G.A. Smith, and N. Osterrieder, *En passant mutagenesis: a two step markerless red recombination system.* Methods Mol Biol, 2010. **634**: p. 421-30.
48. Krause, P.R. and D.M. Klinman, *Efficacy, immunogenicity, safety, and use of live attenuated chickenpox vaccine.* The Journal of Pediatrics, 1995. **127**(4): p. 518-525.
49. Cohen, J.I., et al., *Absence or overexpression of the Varicella-Zoster Virus (VZV) ORF29 latency-associated protein impairs late gene expression and reduces VZV latency in a rodent model.* J Virol, 2007. **81**(4): p. 1586-91.
50. Kinchington, P.R., et al., *Identification and characterization of a varicella-zoster virus DNA-binding protein by using antisera directed against a predicted synthetic oligopeptide.* Journal of Virology, 1988. **62**(3): p. 802.
51. Hong, V., et al., *Labeling live cells by copper-catalyzed alkyne--azide click chemistry.* Bioconjug Chem, 2010. **21**(10): p. 1912-6.
52. Alnuami, A.A., et al., *Oxyradical-induced GFP damage and loss of fluorescence.* Int J Biol Macromol, 2008. **43**(2): p. 182-6.
53. Hay, J., et al., *The effect of phosphonoacetic acid on herpes viruses.* J Antimicrob Chemother, 1977. **3 Suppl A**: p. 63-70.
54. Pahud, B.A., et al., *Varicella zoster disease of the central nervous system: epidemiological, clinical, and laboratory features 10 years after the introduction of the varicella vaccine.* J Infect Dis, 2011. **203**(3): p. 316-23.
55. Lotharius, J., et al., *Effect of mutant alpha-synuclein on dopamine homeostasis in a new human mesencephalic cell line.* J Biol Chem, 2002. **277**(41): p. 38884-94.

56. Scholz, D., et al., *Rapid, complete and large-scale generation of post-mitotic neurons from the human LUHMES cell line.* J Neurochem, 2011. **119**(5): p. 957-71.
57. Eriksson, K.S., et al., *The type III neurofilament peripherin is expressed in the tuberomammillary neurons of the mouse.* BMC neuroscience, 2008. **9**: p. 26-26.
58. Glotzer, J.B., et al., *Microtubule-independent motility and nuclear targeting of adenoviruses with fluorescently labeled genomes.* J Virol, 2001. **75**(5): p. 2421-34.
59. Lau, I.F., et al., *Spatial and temporal organization of replicating Escherichia coli chromosomes.* Mol Microbiol, 2003. **49**(3): p. 731-43.
60. Pecinka, A., et al., *Tandem repetitive transgenes and fluorescent chromatin tags alter local interphase chromosome arrangement in Arabidopsis thaliana.* J Cell Sci, 2005. **118**(Pt 16): p. 3751-8.
61. Dembowski, J.A. and N.A. DeLuca, *Selective recruitment of nuclear factors to productively replicating herpes simplex virus genomes.* PLoS Pathog, 2015. **11**(5): p. e1004939.
62. Dembowski, J.A. and N.A. Deluca, *Purification of Viral DNA for the Identification of Associated Viral and Cellular Proteins.* J Vis Exp, 2017(126).
63. Hoelting, L., et al., *Stem Cell-Derived Immature Human Dorsal Root Ganglia Neurons to Identify Peripheral Neurotoxicants.* STEM CELLS Translational Medicine, 2016. **5**(4): p. 476-487.
64. Zhang, X.M., M. Yin, and M.H. Zhang, *Cell-based assays for Parkinson's disease using differentiated human LUHMES cells.* Acta Pharmacol Sin, 2014. **35**(7): p. 945-56.
65. Rigamonti, A., et al., *Large-Scale Production of Mature Neurons from Human Pluripotent Stem Cells in a Three-Dimensional Suspension Culture System.* Stem Cell Reports, 2016. **6**(6): p. 993-1008.
66. Ziegler, L., et al., *Efficient Generation of Schwann Cells from Human Embryonic Stem Cell-Derived Neurospheres.* Stem Cell Reviews and Reports, 2011. **7**(2): p. 394-403.
67. Assouline, J.G., et al., *Varicella-zoster virus infection of human astrocytes, Schwann cells, and neurons.* Virology, 1990. **179**(2): p. 834-44.
68. Iwamoto, M., et al., *A general chemical method to regulate protein stability in the mammalian central nervous system.* Chem Biol, 2010. **17**(9): p. 981-8.